# Superstructure Optimization of Hybrid Thermal Desalination Configurations

by

Tawfiq Dahdah

BE Mechanical Engineering American University of Beirut, 2011

Submitted to the Department of Mechanical Engineering in partial fulfillment of the requirement for the degree of

Master of Science in Mechanical Engineering

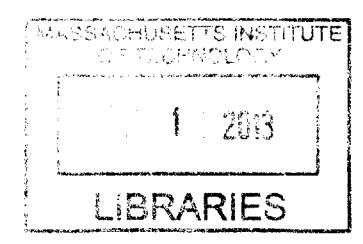
at the

Massachusetts Institute of Technology

September 2013

©2013 Tawfiq Dahdah. All rights reserved.

**ARCHIVES** 



Chairman, Committee for Graduate Students

The author hereby grants to MIT permission to reproduce and to distribute publicly paper and electronic copies of this thesis document in whole or in part in any medium known or hereafter created.

Signature of Author:	
	Department of Mechanical Engineering 30 August 2013
Certified by:	
	Alexander Mitsos Visiting Scientist Thesis Supervisor
Accepted by:	
Ral	David E. Hardt oh E. and Eloise F. Cross Professor of Mechanical Engineering

# Superstructure Optimization of Hybrid Thermal Desalination Configurations

by

### Tawfiq Hanna Tawfiq Dahdah

Submitted to the Department of Mechanical Engineering on August 30, 2013, in partial fulfillment of the requirements for the degree of Master of Science in Mechanical Engineering

### Abstract

As the global demand for freshwater continues to increase, a larger number of resources are dedicated to seawater desalination technologies. In areas with high temperature and salinity water, thermal desalination technologies are often employed. In other areas, reverse osmosis technologies are more popular. While both these technologies have witnessed improvements in recent years, economic and performance issues still pose significant barriers to their universal implementation, which has left many countries, including ones bordering oceans and seas, suffering from dire water scarcity issues. This thesis proposes a methodology which enables the identification of improved thermal-based desalination structures. It is based on the notion of superstructure, which allows for the representation of numerous feed, brine and vapor routing schemes.

A superstructure is developed. By adjusting the flow routings, the superstructure is capable of representing the common thermal desalination structures, as well as an extremely large number of alternate structures, some of which might exhibit advantageous behavior. The superstructure is built around a repeating unit which is a generalization of an effect in a multi-effect distillation system (MED) and a stage in a multi-stage flash system (MSF). Allowing for just 12 repeating units, more than 10<sup>40</sup> different structures can be represented. The superstructure is thus proposed as an ideal tool for the structural optimization of thermal desalination systems, whereby the optimal

selection of components making up the final system, the optimal routing of the vapors as well as the optimal operating conditions are all variables simultaneously determined during the optimization problem. The proposed methodology is applicable to both stand-alone desalination plants and dual purpose (water and power) plants wherein the heat source to the desalination plant is fixed. It can be extended to also consider hybrid thermal-mechanical desalination structures, as well as dual purpose plants where the interface of power cycle and desalination is also optimized for.

A multi-objective structural optimization of stand-alone thermal desalination structures is performed in Chapter 2, whereby the performance ratio of the structures is maximized while the specific area requirements are minimized. It is found that for any particular distillate production requirement, alternate structures with non-conventional flow patterns require lower heat transfer areas compared to commonly implemented configurations. Examples of these non-conventional configurations are identified, which include a forward feed forward feed MED structure, involving the integration of two forward feed MED plants.

Chapter 3 highlights how the superstructure can be adapted to optimize integrated thermal desalination and thermal compression systems. Specifically, the conducted study investigates whether there is any merit to the thermal compression of vapor streams produced in intermediate MED effects as opposed to the common practice of compressing vapors produced in the last effect. The study concludes that intermediate vapor compression results in significant reductions in area requirements, as well as significant increases in maximum distillate production capacities. Moreover, the study confirms that the optimal location of vapor extraction is heavily dependent on the exact distillate production requirement in question. Two novel configuration forms are informed by the optimization. The first is an integrated MED-TVC + MED + MSF system, while the second is an integrated MED-TVC + MSF system.

### Acknowledgments

As my MIT experience comes to a close, I would like to thank some of incredible individuals I was fortunate to have met along the way.

Professor Alexander Mitsos, I owe you a tremendous amount of gratitude for opening up this life-changing experience for me and warmly welcoming me into your lab. Thank you for allowing me the opportunity to work on a very meaningful project to tackle water scarcity. This is a global problem, which I now feel strongly attached to, and one that I hope to continue involving myself in even as I leave technical engineering. I thank you for your thoughtful discussions, for your constant motivation and for always pushing me towards realizing my fullest potential. I admire both your work ethic and your strong sense of family. You always lead by example and I wish you all the best in your career.

Enrique, Angelos, Hadi, Abhishek, Annelies, Ragheb, Gina and Surekha, thank you for being wonderful labmates. I relished both our academic and non-academic conversations inside and outside the lab. They have been enlightening, and I have learned a lot from each of you. I consider you all to be my family here in the US and I hope we continue to be lifelong friends even as professional life takes us to different parts of the globe.

To all my friends here in MIT and Boston, thank you for all the experiences we shared together: the crazy overnights, the 3 a.m. runs, the early morning winter swims and the food eating contests just to name a few. I am lucky to have adventurous friends with contagious passions to making a difference. I am hopeful that all of you will be able to accomplish your ambitious goals whatever they may be. I already look forward to our reunions, and recounting all our joyful experiences together.

To Hannah, thank you for all the wonderful times: from 'forcibly' taking me to museums and symphonies, teaching me how to cook, educating me in the arts to uselessly trying to teach me Swedish. You will always be an adventurous kid at heart even when you're 90.

To my dad and mom, I love you both infinitely. This entire thesis is dedicated to you and for the hard work that you put into raising me, Tala, Bana and Majd. Not a single day passes where I don't acknowledge all the love and support you have provided and continue to provide. Dad, thank you for being

my number one idol. Mom, thank you for always reminding me that there is so much else to life other than academics and for being the most optimistic smiley person I know. To my sisters, and brother, thank you for everything. To my aunts, who have graciously welcomed me to their homes, thank you.

Finally, I would like to thank the King Fahd University of Petroleum and Minerals in Dhahran, Saudi Arabia, for funding this work through the Center for Clean Water and Clean Energy at MIT and KFUPM under project number R13-CW-10.

## Contents

1	Intr	oducti	on	15
	1.1	Pressi	ng need for desalination	15
	1.2	Break	down of current desalination technologies	16
	1.3	Thesis	outline	18
2	A fl	exible	superstructure to represent hybrid thermal config-	
	ura	tions		21
	2.1	Introd	uction	21
		2.1.1	Superstructure concept for optimizing thermal desalina-	
			tion structures	24
	2.2	Descri	ption of Conventional Thermal Desalination Processes	26
	2.3	3 Superstructure proposed for the process		28
		2.3.1	Design options	29
		2.3.2	Post-processing to identify optimal hardware	32
		2.3.3	Representation of conventional configurations	34
		2.3.4	Limitations of superstructure	34
		2.3.5	Mathematical representation	35
		2.3.6	Operational Constraints	37
		2.3.7	Optimization variables	37
	2.4	Case s	tudies involving stand-alone thermal structures	39
		2.4.1	Problem Definition	40
		2.4.2	Software and solution methodology	41
		2.4.3	Case study 1: Testing Different Design Specifications	43

		2.4.4	Case study 2: Identifying optimal structures depending	
			on location	46
		2.4.5	Case study 3: Investigating influence of RR $\dots$	47
		2.4.6	Examples of optimal structures	49
		2.4.7	Conclusions	52
3	Ider	ntifying	g Hybrid Configurations Involving TVC	<b>55</b>
	3.1	1 Introduction		55
	3.2	2 Problem definition		58
	3.3	Model	ing	59
		3.3.1	The thermal desalination superstructure	59
		3.3.2	Integration with steam ejector	61
		3.3.3	Model of the steam ejector	62
	3.4	Optim	ization	64
		3.4.1	Objective function	64
		3.4.2	Optimization methodology	66
		3.4.3	Constraints to allow justified comparison of different struc-	
			tures	67
	3.5	Result	s and discussion	68
		3.5.1	Intermediate vapor extraction increases maximum pos-	
			sible GOR	68
		3.5.2	Lower area requirements for structures with intermedi-	
			ate vapor compression	72
		3.5.3	Optimal hybrid structures	74
		354	Flowsheets of ontimal hybrid structures	75

	3.5.5	Advantages of hybrid structures	8
3.6	Conclu	asion	0



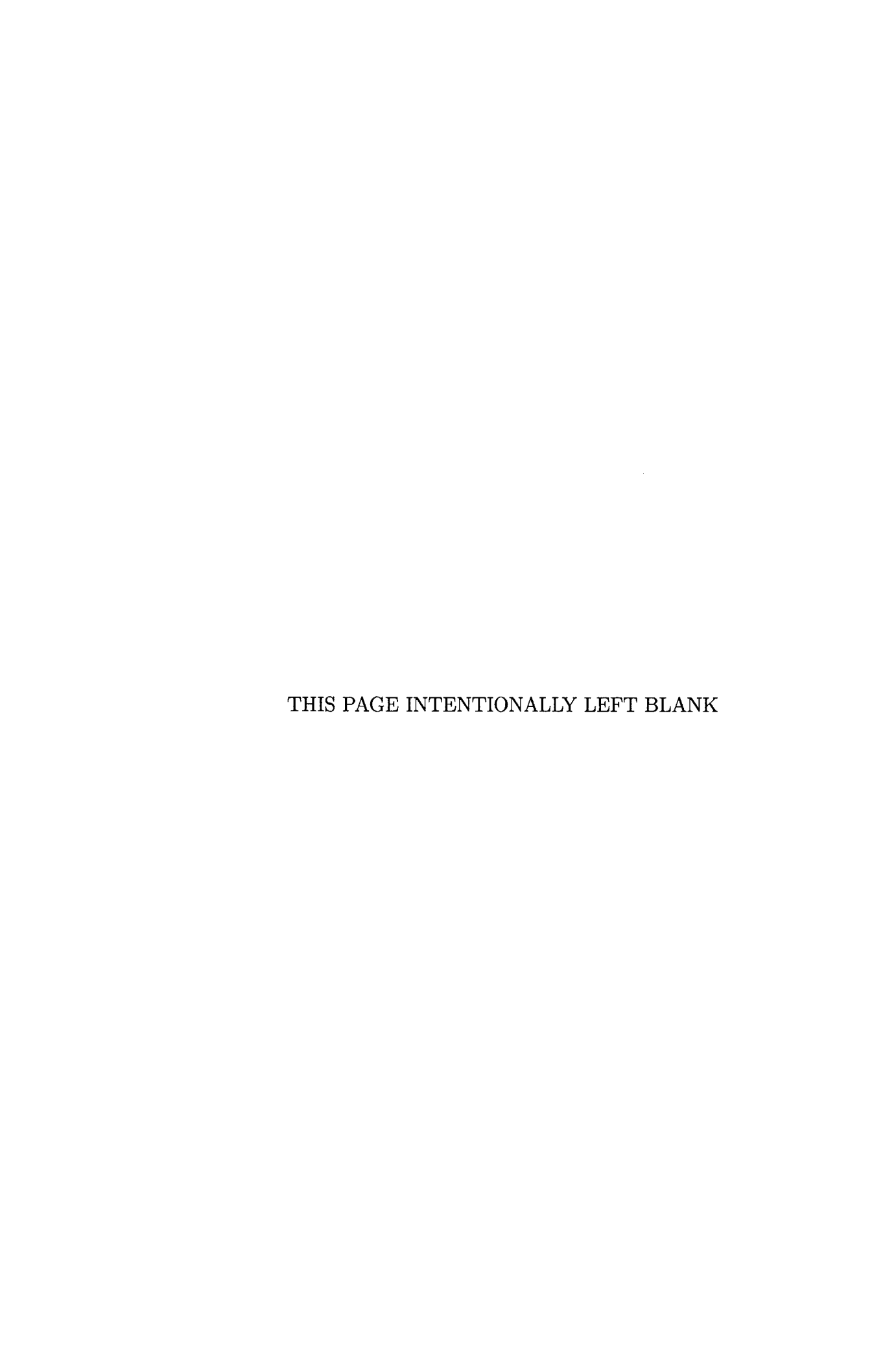
## List of Figures

1	Generalized superstructure illustrating different brine and feed	
	routings. Without loss of generality, 12 repeating units are	
	shown. Vapor routings are shown in Figure 2	30
2	Representation of the repeating unit $i$ of the proposed super-	
	structure, demonstrating vapor, feed and brine alternate routings	31
3	Comparison of minimum SA requirements $(m^2/(kg/s))$ for dif-	
	ferent recovery ratios for 4 distillate production amounts	48
4	Optimized configuration for PR = $8.75$	49
5	Optimized configuration for $PR = 10.25$	50
6	Optimized configuration for $PR = 11 \dots \dots$	50
7	Superstructure capable of representing different combinations of	
	MSF , MED and feed preheater combinations. Vapor routings	
	are not represented in this schematic	61
8	Example of FF MED - TVC configuration with vapor extracted	
	from last effect. Only a fraction of the vapor generated in last	
	unit needs to be condensed in the down-condenser	62
9	Example of a FF MED-TVC with vapor extracted from an in-	
	termediate (6th) effect. Only a fraction of vapor produced in	
	the 6th unit is directed towards feed pre-heating and vapor pro-	
	duction within the next (7th) unit	63
10	Illustrution of example of an MED-TVC $+$ MED $+$ MSF with	
	vapor extraction at $N=4$	77
11	Labeling of different flow streams	78

12	Illustrution of an example of an MED-TVC + MSF with vapor	
	extraction at $N=8$	78
13	A 12 effect forward feed (FF) MED, from a simplified super-	
	structure. (Brine and feed streams only)	83
14	A 12 effect Parallel Cross (PC) MED, from a simplified super-	
	structure (Brine and feed streams only). Brine flash boxes can	
	be recursively removed to simplify to traditional PC MED	83
15	A 12 stage once through MSF, from a simplified superstructure.	
	(Brine and feed streams only). Vapor generated in flash boxes	
	is used to pre-heat the feed	84
16	Simplified block diagram to illustrate make up of maximum	
	GOR structure for $ES = 6$	94
17	Simplified block-diagram to illustrate make up of maximum	
	COR structure for $FS = 0$	04

## List of Tables

1	Comparison of minimum SA requirements $(m^2/(kg/s))$ for dif-	
	ferent design specifications for $PR = 10, 10.5, 11$ and $11.25$ for	
	$T_{sw}=25$ °C, Salinity = 4.2 g/kg, RR = 0.41	45
2	Comparison of minimum SA requirements ( $m^2/(kg/s)$ ) for dif-	
	ferent locations of seawater extractions; RR = 0.38, $T_{HS_{input}}$ =	
	70° C	47
3	Choice of parameters for present study including motive steam	
	and seawater conditions	59
4	Properties of maximum GOR structures for the different vapor	
	extraction locations	69
5	Comparison of minimum SA $(kgs)/(m^2)$ at different GOR for	
	different ES	72
6	Properties of optimal structures for GOR = 15 for different	
	vapor extraction locations	73
7	Optimal structures corresponding to different ES for $GOR = 15$	75
8	Optimal structures corresponding to different ES for maximum	
	GOR	75



### 1 Introduction

### 1.1 Pressing need for desalination

The global demand for a steady, economical supply of fresh water continues to increase. This trend is driven on the one hand by surging population growth, and on the other hand by economic development, industrialization and an expansion of irrigation agriculture, all of which demand fresh water [1, 2]. Although there is currently enough fresh water for the planet's 7 billion inhabitants, there is a high unevenness in its distribution, which has left an increasing number of regions chronically short of water [3]. In these water-stressed regions, numerous alleviating actions have been taken including constructing more water catchment areas, building improved water distribution networks, along with improved water conservation measures. While these measures do result in better utilization of the constrained freshwater resources, they do not guarantee sufficient water for all. One of the main known modes of increasing the existing water supply is seawater desalination; a proven process that can reliably convert the seemingly limitless supply of seawater to high-quality water suitable for human consumption. Already, desalination plants operate in more than 120 countries in the world, including Saudi Arabia, the United Arab Emirates, Spain, Greece and Australia.

While large-scale desalination plants have been available for a long time, further installations are expected to increase at an alarmingly fast rate, with most of the desalination plant installations expected to be of either the thermal or membrane type. It is projected that by just 2016, the global water production by desalination will increase by more than 60 percent from its value in 2010 [4].

### 1.2 Breakdown of current desalination technologies

Reverse osmosis (RO) plants, the primary membrane-based technology, have gathered tremendous installation momentum in the past years owing mostly to their increased cost savings; in part owing to the development of cheaper, longer lasting membranes and in part owing to reduced energy requirements. In the last decade alone, the required electrical power to drive RO plants has decreased by more than 50 percent [5]. This decrease in energy consumption is accredited to continuous technological advances, including higher-permeability membranes, improved energy recovery devices, and the use of more efficient pumps. Current state-of-the-art RO technologies require significantly lower energy requirements compared to all other desalination technologies, and have emerged as the standard against which the energy efficiency of all technologies - including thermal technologies - are compared. It is thus not surprising that RO currently dominates the global desalination market, accruing approximately 50 - 60 percent of the overall market share [6].

Although thermal based technologies - comprised mostly of multi-stage flash distillation plants (MSF) and multi-effect distillation plants (MED) - occupy a smaller fraction of the world market, they dominate the Middle Eastern market where they occupy 75 percent market share. There are several con-

tributing factors to this apparent deviation from global trends. One decisive factor is the region's noticeably low energy costs. The unit product cost, based on which designers usually select the preferable desalination technology, is thus less sensitive to energy requirements - which are usually lower in RO - and are more geared towards capital costs which are lower in thermal desalination. The high salinity and temperature levels of the Arabian Gulf, from which most of the region's plants extract feed-water, is another important factor. While increased feed-water salinity only indirectly affects performance of thermal desalination plants by restricting the maximum recovery ratio, it severely cripples the performance of the salinity-sensitive RO system. Increases in the feed-water salinity into the RO system translate into increased pretreatment costs, increased membrane replacement costs, alongside increased pumping requirements. Moreover, the regions elevated feed-water temperatures, while positively affecting the performance of thermal desalination through reducing feed pre-heating requirements, negatively affects RO systems by increasing salt passage and increasing the risk of bio-fouling, which more than countereffects the increased permeability with higher temperature [7]. Other reasons encouraging regional adoption of thermal desalination systems include the convenience of integration with pre-existing power plants, as well as the accumulated field experience that increases the technology's controllability, operability and reliability [8].

### 1.3 Thesis outline

The water scarcity problem is by no means restricted to arid areas. Even in industrialized nations currently considered water-rich, contamination of freshwater resources coupled with global warming effects that include reductions in snow-melt and the loss of glaciers are threatening to result in water scarcity within the coming decades, if not sooner [9]. Thus the need to develop efficient and economical desalination technologies capable of bridging the widening gap between the supply and demand of high-quality water is a pressing global problem necessary to guarantee a stable world future [10, 11].

This thesis is specifically devoted to the optimization of thermal-based desalination structures. Chapter 2 examines pure thermal desalination structures, while Chapter 3 studies thermal structures integrated with thermal vapor compression units. Some repetition between the chapters is done so that the chapters are more or less contained. The overall goal throughout is to clearly identify novel structures that improve upon conventional existing configurations, to quantify their improvements through a comparison of several key metrics, and finally to detail sample flowsheets to hopefully benefit the designers of next generation plants many of which will likely be of the thermal type. To aid in identifying novel structures, the concept known as a superstructure is utilized. The general notion of a superstructure, coupled with its capabilities and advantages are detailed in Chapter 2. The proposed methodology is applicable to both stand-alone desalination plants and dual purpose (water and power) plants wherein the heat source to the desalination is fixed.

It can be extended to also consider hybrid thermal-mechanical desalination structures, as well as dual purpose plants where the interface of power cycle and desalination is also optimized for.



## 2 A flexible superstructure to represent hybrid thermal configurations

### 2.1 Introduction

Given the urgent need to constantly improve thermal desalination plants, authors seeking to contribute to the improvements in this field, have undertaken various approaches.

Several authors, through parametric studies, investigated the influence of numerous variables to gauge their relative importance on performance of MED plants [12, 13, 14, 15, 16]. These variables include the total number of effects, the temperature and salinity of the incoming feed, the temperature of the heating steam, as well as the temperature of the evaporator in the last effect. While such studies occasionally provide useful insights, most of the relationships that arise, e.g. distillate production is heavily dependent on the number of effects, are mostly expected. Moreover, the results of such studies are of limited use to designers, mainly because parametric studies do not consider interaction between the different system variables. The need for optimization is clear.

To optimize thermal desalination plants, authors have resorted to differing objective functions. In certain situations, the objective functions are economic related such as minimizing unit product cost or minimizing specific heat transfer areas. In others, the objectives are tied to the thermodynamics such as

maximizing distillate production or exergy efficiency [17, 18, 19]. While single objective functions are frequently resorted to, multi-objective optimizations are generally preferable. The main reason is that single objective optimization does not necessarily yield applicable designs. For instance, if the distillate production is maximized as part of a single objective study, the associated costs are not directly considered. The result is generally an uneconomical unimplementable plant. In contrast, multi-objective optimization studies can consider both efficiency and economic measures, resulting in more realistic designs. Further, multi-objective optimization allows the quantification of the trade-offs between competing criteria.

The works directed to improve thermal desalination have taken numerous fronts. Some authors have considered the stand-alone optimization of thermal-based configurations. While some of these authors optimized operating conditions associated with pre-existing configurations, others proposed alternative schemes - such as the MSF-MED proposed in [20, 21] - which they subsequently optimized and compared to conventional structures. Other authors meanwhile have examined hybrid thermal-membrane based technologies seeking to make use of the ease of their integration. By suggesting alternative flow routing possibilities, authors propose that the resulting hybridized structures offer significant synergetic benefits. These advantages include, but are not restricted to, the reduction of capital costs through use of common intake and outlet facilities, the potential for reduced pretreatment and an increase in top brine temperature in thermal desalination [22, 23, 24, 25, 26, 27, 28]. Other

authors propose integrating thermal desalination configurations with thermal vapor compression systems as an efficient means of increasing total distillate production, reducing cooling water requirements and potentially reducing heat transfer area requirements, all while being characterized by simple operation and maintenance [29, 30].

While the aforementioned contributions have resulted in more efficient desalination plants with improved economics, one significant drawback impedes even larger improvements. The general practice of fixing both the hardware involved in a plant, as well as its flowsheet prior to optimization has obvious shortcomings. It can be easily seen that such an approach is inferior to an alternate optimization approach whereby both the hardware and the flowsheet could be modified during the optimization process. This is especially true since there is no guarantee that any of the common configurations already proposed in literature is optimal under any conditions. For studies concerning hybrid plants in particular, the more flexible optimization could yield breakthroughs as there might be significant benefit from deviating from the conventional setups specific to stand-alone structures.

The general need to investigate modifications in hardware and flow patterns has been looked into. Authors generally proceed to propose a series of modifications they envision to be advantageous. They subsequently optimize the resulting arrangements, and compare the results to those exhibited by conventional structures to decide on the merit-worthiness of their ideas. Unfor-

tunately, such a series of steps is time consuming and their success in yielding improved results depend highly on both the author's experience and creativity. This method is further restrictive because the testing of the huge number of combinations of different possible flowsheets and hardware is infeasible.

# 2.1.1 Superstructure concept for optimizing thermal desalination structures

In this chapter, we propose a flexible tool that is capable of adjusting the process diagram of thermal desalination configurations. The tool, which is based on the concept of a superstructure, is able to adjust the hardware component set, the routing of all the different flows entering and exiting each of the eventual components making up the system, as well as adjusting the sizing of all the necessary components. Through this process, the tool can represent all the existing thermal desalination configurations, in addition to an extremely large number of alternative configurations, which indicates that the proposed tool is ideal for the systematic comparison of alternatives and the generation of new ones. Note that the superstructure is a notion employed in process design that illustrates all the different hardware and connectivity possibilities to be considered for optimal process design [31].

The tool allows for improved optimization studies involving thermal configurations. Further, it can be easily adjusted to be used in optimization studies of hybrid configurations involving membrane based technologies and thermal vapor compression systems. The tool can be modified to investigate

co-generation by integrating it with a power plant model. To illustrate the usefulness of the proposed tool, the results of several multi-objective optimization studies are presented, whereby the performance improvements are quantified, while the optimal flow patterns are shown to deviate from the convention.

While the origin of the superstructure approach is in the chemical process industry, authors have recently utilized it in the field of desalination. Zak and Mitsos [32], by identifying physical processes shared by all thermal desalination technologies, constructed a superstructure capable of representing existing thermal desalination configurations as well as novel ones, however did not optimize it. Sassi et al. [33] used it to identify optimal RO networks for a variety of differing temperatures and salinities. The study confirmed, as expected, that such factors have a significant impact on the subsequent optimal design and operation. Skiborowski et al. [34], on the other hand, optimized a superstructure considering the combination of an RO network with an MED configuration specified to be of the forward feed type. Again, the work demonstrates that optimal configuration varies depending on local factors such as the energy costs and pretreatment costs. As a final example, Mussati et al. [35, 36, 37] used a superstructure for varying purposes including identifying optimal coupling of power and desalting plants and identifying improvements in the design of MSF plants.

# 2.2 Description of Conventional Thermal Desalination Processes

The process of constructing a general superstructure to represent thermal desalination structures is greatly facilitated by the fact that both MED and MSF operate on the same fundamental principles. Both processes require an external heat input to drive the initial production of vapor, and an external work input to drive the pumps which are needed to overcome the different pressures losses experienced by the flows.

In MED, the external heat input is used to first sensibly heat the incoming feed to the first effect and subsequently evaporate a portion of it. Two separate streams consequently exit the effect: a more concentrated brine stream, and a saturated vapor stream. The saturated vapor is split; a portion of it is used to pre-heat the feed in a counter-current feed preheater while the remaining portion is used as heating steam to the next effect where additional vapor is generated. To allow for the vapor produced in one effect to heat the contents of the next effect, a decreasing pressure profile within consecutive effects is necessary. A similar procedure is repeated in each of the remaining effects whereby a portion of the vapor generated in the previous effect is used to convert a portion of the feed entering into the effect into vapor. Within the last effect, all the generated vapor is directed towards pre-heating the feed in a down condenser. However, since the incoming feed is generally not capable of carrying away all the heat required to condense the inputted vapor, additional cooling water is usually entered into the down condenser, where it is

pre-heated and subsequently rejected back to the sea. To recover additional energy in the system, intermediate brine and distillate streams are flashed as they are successively entered into lower pressure chambers.

The source of feed to each effect varies depending on the configuration employed. In the forward feed (FF) MED configuration, all of the feed entering into the system is directed solely to the first effect. No intermediate feed extractions occur as the feed leaves each consecutive preheater, but rather all the feed leaving a particular preheater is inputted into the subsequent one. For all the remaining effects, the feed to the effect is comprised of brine exiting from the previous effect. FF is typically advantageous since the brine leaving the highest temperature effect is the least saline; a characteristic that reduces the risk of scaling. The parallel cross (PC) MED configuration, is an alternate configuration. Within this configuration, the feed to each effect is comprised of pre-heated seawater extracted at the outlet of the corresponding feed pre-heater. Brine exiting each effect is simply flashed to produce additional vapor, without allowing any of the brine to be inserted as feed into any of the subsequent effects. Typically the PC-MED configuration is found to be capable of larger distillate production capabilities compared to FF-MED [38].

MSF largely resembles the MED configuration in its flowsheet with the exception that all the vapor generated in any particular stage is solely directed towards pre-heating the feed in the next unit. As a consequence, no vapors are generated by evaporation in MSF. Interestingly, MSF can be considered to be

a more specific and constrained form of MED including flash boxes. The main mode of vapor production in MSF is the process of brine flashing, a process which is possible because of the decreasing pressure profile within consecutive stages. However, some additional vapor does form by flashing condensed distillates. For the same number of repeating units, MSF is characterized by significantly lower recovery ratios (RR), as compared to MED due to the lower thermodynamic efficiency of flashing compared to boiling. MSF has however the advantage that since the top operating temperature can reach up to approximately 110°C compared to approximately 70°C in MED, which allows for a larger number of stages in MSF as compared to the number of possible effects in MED. The brine leaving the last stage of the MSF can be returned to the sea as brine blow down, a configuration known as once through MSF (MSF-OT). Alternately, some designers choose to mix a portion of the brine leaving the last stage with the incoming feed to the plant; a configuration known as MSF with brine mixing (MSF-BM).

### 2.3 Superstructure proposed for the process

The superstructure was constructed with the constraint that all of the resulting process designs can be physically implemented. The finalized superstructure is represented in Figure 1. Section 2.3.1 discusses all the different design options allowed by the process, while Section 2.3.2 examines how variables can be manipulated to delete different components. Section 2.3.3 highlights, with the aid of schematics, how the generalized superstructure can be reduced to known configurations. Section 2.3.4 discusses the main limitations of the

current superstructure. Sections 2.3.5 outline details of the mathematical modeling of different components that could potentially make up the final system. Lastly, Sections 2.3.6 and 2.3.7 outlines the necessary operation constraints, as well as the choice of optimization variables.

#### 2.3.1 Design options

Several novel flow patterns are allowed. Figure 1 provides a schematic illustrating the numerous brine and feed flow routings in the superstructure proposed. For simplicity a total of 12 units is chosen. To maintain a non-convoluted figure, the vapor routings barring the input primary heating steam are not shown in Figure 1. Figure 2, however, provides the complete schematic including vapor routings for a sample repeating unit i in the superstructure. A few exemplary design options allowed by the superstructure are also represented in Figure 2, indicated by the variables  $(\alpha, \lambda \text{ and } \epsilon)$ .

The superstructure is built around several discrete/continuous choices:

The choice of what fraction of the overall feed flow leaving any intermediate feed preheater (FPH) is extracted to be sent to the corresponding MED effect ( $\epsilon$ ) and what fraction is directly sent to the next preheater (1-  $\epsilon$ ). This is a continuous decision where the condition ( $\epsilon$  = 1) corresponds to complete extraction, while ( $\epsilon$  = 0) signals that all feed leaving a preheater is inserted to the next preheater. Any intermediate value corresponds to only a fractional extraction. At the exit of the down-condenser, there is an additional split variable  $\epsilon_1$ , shown in Figure 1,

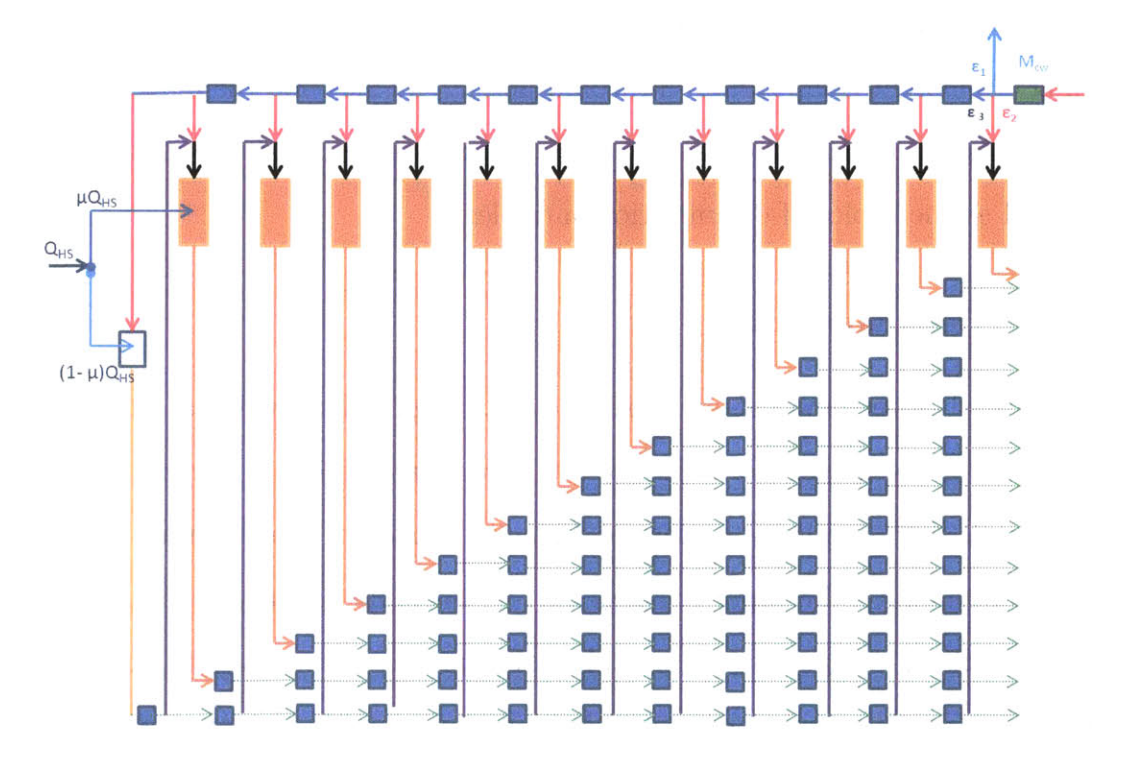


Figure 1: Generalized superstructure illustrating different brine and feed routings. Without loss of generality, 12 repeating units are shown. Vapor routings are shown in Figure 2.

which dictates what fraction of total feed is returned to the sea (i.e serves as cooling water). The fractions  $\epsilon_2$  and  $\epsilon_3$  then dictate the corresponding fractions that are entered into last effect and fed to the last preheater respectively.

The choice of what fraction of the total brine leaving a particular brine flash box, is extracted to be fed to the next effect  $(\lambda)$  and what fraction is allowed to be sent to the next flash box in the same flash box line  $(1-\lambda)$ . This feature allows the model an interesting option of using brine outputted from any effect i as feed to any effect j, where j > i.

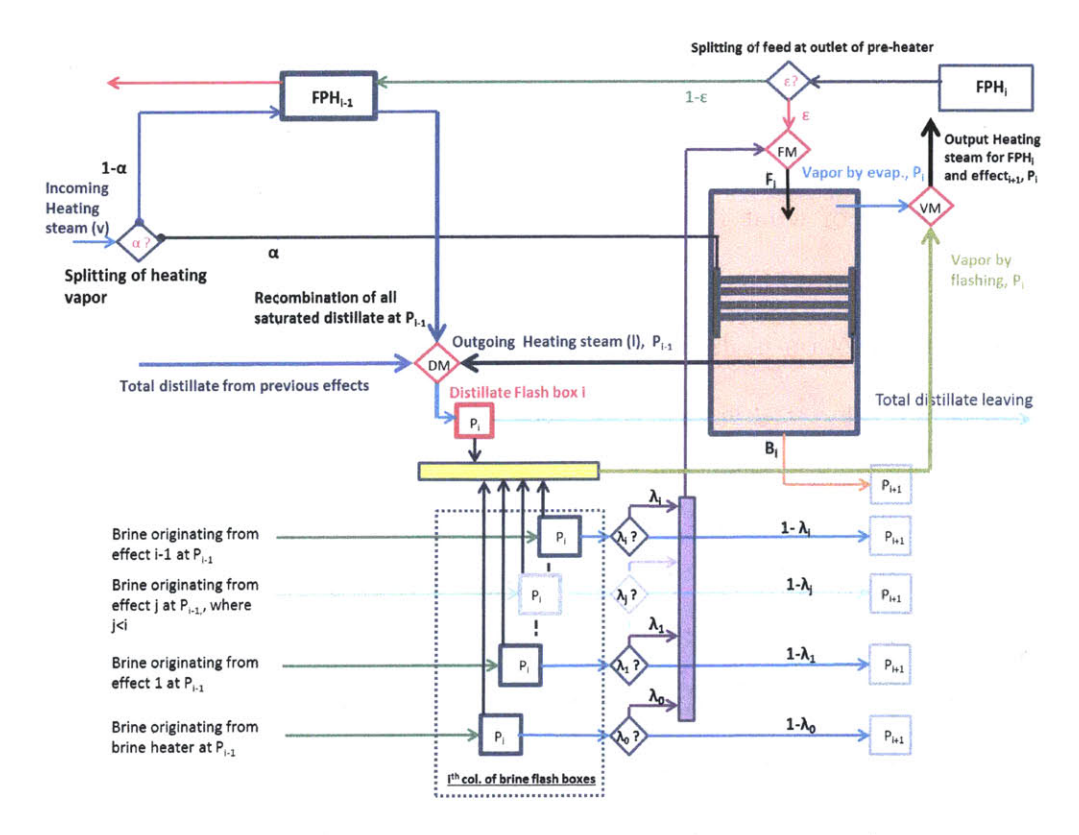


Figure 2: Representation of the repeating unit i of the proposed superstructure, demonstrating vapor, feed and brine alternate routings

The choice of what fraction of the available secondary heating steam (comprised of vapors produced by brine evaporation, brine flashing, and distillate flashing) is sent to the next effect ( $\alpha$ ) to accomplish brine evaporation, and what fraction is sent to the corresponding feed preheater to achieve feed pre-heating (1- $\alpha$ ). In literature, designers often allocate all the vapor formed by brine flashing towards the end of feed pre-heating, and fix all the vapors formed within an effect towards the end of heating contents of the next effect. By combining all the formed vapors, and subsequently choosing a value for  $\alpha$ , some of the vapor formed by brine flashing could be used towards brine evaporation within next effect, while

some of the vapor formed by evaporation within an effect could be used towards feed pre-heating in the next unit of superstructure.

- The choice of what fraction of the primary heating steam available is directed towards the 1st MED effect for evaporation ( $\mu$ ) and what remaining fraction is directed towards the brine heater corresponding to the MSF line (1- $\mu$ ) is shown in Figure 1.

For the example of 12 effects, optimization of the superstructure has to ultimately decide on the optimal values for each of the 13  $\epsilon$ 's, 72  $\lambda$ 's, 12  $\alpha$ 's and 1  $\mu$  variables. In total these 98 different variables dictate a very large combination of possible hardware components, and combination of possible finalized flowsheets (in excess of  $10^{40}$  structures).

### 2.3.2 Post-processing to identify optimal hardware

The general superstructure made up N repeating units is capable of representing a maximum of N effects, N feed preheaters, N-1 distillate flash boxes and a maximum of  $N^2/2$  different brine flash boxes. The superstructure is flexible in adapting what subset of allowable components are ultimately used. One interesting and extremely useful feature of the implementation is that components can be deleted without the need to resort to any integer variables which is the traditional method of implementing superstructures as in [37, 39, 40]. Avoiding the use of integer variables greatly minimizes the relative difficulty of system optimization, which the superstructure will eventually be used for.

Assuming the optimization is complete, a thorough post-processing of the value of the different system variables signals whether a component is included. Deletion of an effect is signaled either by the absence of any incoming feed into the effect, or alternately by the absence of any vapor production by evaporation within the effect. Deletion of a preheater component is indicated by the absence of any heating vapor being directed towards it (i.e., the corresponding  $\alpha=1$ ), which is synonymous to an absence of any temperature difference as the flow passes through the device; a sign that no heat transfer occurred. For brine and distillate flash boxes, elimination of the hardware is signaled by the absence of an incoming flow into the component. Tolerances are needed to help deciding when a particular flow can be neglected. In this work, the assumption is that any flow-rate that does not exceed 0.05 kg/s is negligible.

While the superstructure is capable of representing N<sup>2</sup>/2 different brine flash boxes, it can be envisioned that capital costs associated with that many separate components would be tremendously high. Fortunately, the number of brine flash boxes can be manually reduced in the post-processing phase through a recursive sequence. A group of brine flash boxes operating at a common pressure can be combined into one equivalent operating flash box operating at the same pressure if all of their outputs are redirected to the same location to mix. This process is repeated until no two differing brine flash boxes operating at the same pressure feed all their output into the same location.

### 2.3.3 Representation of conventional configurations

Through an appropriate choice of extraction variables, the superstructure may be reduced to known structures. For illustrative purposes, the process diagrams for the FF-MED (Figure 13), the PC-MED (Figure 14), and the OT-MSF (Figure 15) are figuratively represented, whereby the transparency of the streams and components signal their exclusion. These figures are found in Appendix A. It is worth highlighting that the intermediary heating steams are not shown in the schematics. The procedure, however, is to combine all the vapor streams formed by all the different modes of vapor production to form an overall heating steam, which is subsequently split appropriately among the feed heater and effect.

#### 2.3.4 Limitations of superstructure

In general, a superstructure represents all the options that the authors perceive to be potentially advantageous. Herein, the superstructure does not allow the option of the backward feed which is considered disadvantageous; the process of redirecting brine outputted from an effect to a higher pressure prior effect. A configuration characterized by backward feed has an increased risk of scaling since the highest temperature effects are also characterized by the highest salinities. Moreover, the brine exiting an effect would have to be pumped from one effect to the next which would significantly increase pumping requirements.

Within the last effect certain options such as the recirculation and mixing

of part of the brine blow down with incoming feed are not represented. This is a common procedure in MSF configurations. However, since only 12 units of the superstructure are implemented in this work, the dominant structures are expected to take the form of MED structures, where this option is not common. Nevertheless, it would be interesting to investigate whether such an idea has merit in future versions of the superstructure.

The mathematical model computes most of the important metrics including the RR (defined as the fraction of the feed converted to distillate), the performance ratio and the specific area requirements. An accurate determination of the geometry of the individual components, however, is not computed in this work. As a result, pumping requirements which themselves are heavily dependent on geometry, are not accurately determined.

#### 2.3.5 Mathematical representation

A detailed description of the mathematical modeling of the different system components which include the effects, preheaters, flash boxes, mixers and splitters is provided in Appendix B. The mathematical modeling is based on mass, species and energy balances around each of the components. Appendix C describes how the heat transfer requirements within the effects and preheater are determined, while Appendix D outlines the main assumptions utilized in this model.

Appendix B provides the general equations defining how mixers and split-

ters operate. It is clear, however, by inspecting Figures 1 and 2 that numerous mixers and splitters occur within the overall system. Three different instances of mixing occur within any particular superstructure unit, indicated in Figure 2. A feed mixer (denoted in Figure 2 as FM) allows the formation of the total feed to an effect by allowing the blending of several brine streams extracted from the appropriate flash boxes with extracted feed exiting from a preheater. A vapor mixer (denoted in Figure 2 as VM) combines all generated vapor streams produced in a particular unit to form the overall heating to the next unit of the superstructure. Finally, a distillate mixer (denoted in Figure 2 as DM) merges the condensed heating steam with the combined distillate produced in prior units. The distillate outputted from DM is inputted into an appropriately pressured distillate flash box where it flashes.

Splitters, on the other hand, can be seen to occur at multiple system locations which include the outlet of the down condenser, the outlet of each of the preheaters as well as the outlet of each of the brine flash boxes. A further splitter divides the input heating steam so that a fraction of it can be directed to heat contents of the first effect, while the remainder is directed to the brine heater. Further splitters occur at the outlet of the each of the VMs to segregate the vapor to be used for feed pre-heating from the vapor to be used for evaporation within the appropriate effect.

#### 2.3.6 Operational Constraints

To ensure the feasibility of the finalized structure, several temperature constraints need to be enforced. The constraints include:

- Saturation temperature of the brine decreases with effect number.
- The temperature of the heating steam exceeds the temperature of the feed it is used to heat at both the outlet and inlet of each preheater.
- The saturation temperature of the heating steam is greater than the saturation temperature of the brine within the effect it is designated to heat.
- The temperature of the feed exiting a preheater is not less than the temperature of the feed entering a preheater.
- The temperature of the cooling water leaving the down condenser does
   not exceed the temperature of the vapor generated in the last effect.

Although it is customary to set minimum pinches in heat exchangers, this work avoids doing so. Since one of the objective functions will always include an economic related metric, the optimizer will itself seek a solution where sufficiently large temperature differences between the heating and heated medium are always made available.

#### 2.3.7 Optimization variables

In all subsequent optimization studies performed using the superstructure, the optimization variables include a subset of the variables to be discussed herein. The first set of optimization variables are the split ratios discussed in Section 2.3.1, which are considered to be continuous, with possible values ranging from 0 to 1. The other potential optimization variables are the overall feed flow rate to system, the saturation temperature within each of the effects, as well as the temperature profile of the feed at the inlet and outlet of each of the preheaters. A setup where all the aforementioned variables are not preset in any way prior to the optimization will from hereupon be referred to as unconstrained superstructure optimization.

Once the value of all the optimization variables are determined, simple mass and energy balances can be used to determine the flow rates and concentrations of all the brine, feed and distillate streams within the system. The different thermodynamic losses and overall heat transfer coefficients can then computed, which allow the determination of the required sizing of each of the system components.

While optimization of the unconstrained superstructure is always expected to yield the best results, the superstructure can be used in alternative investigations where some of the optimization variables are input into the problem as fixed parameters. For instance, to identify the optimal operation conditions associated with a conventional PC-MED or FF-MED configuration, all the split ratios are specified as parameters to the optimization problem. Further uses of the superstructure will be illustrated in several case studies presented in Section 2.4.

### 2.4 Case studies involving stand-alone thermal structures

This section intends to highlight the wide capabilities of the superstructure through three illustrative case studies. All the case studies considered herein deal with optimization of standalone thermal configurations. The main intention of the first case study is to illustrate how optimization of the superstructure yields significantly improved configurations relative to the conventional thermal configuration restricted by conventional design specifications. Further, the study shows that even if the choice of plant is restricted to one of the conventional designs, the optimal design is heavily dependent on many factors including distillate production requirements. The second case study, presented in Section 2.4.4, examines the effect of the temperature and salinity of the incoming feed-water on the resulting optimal structures. The study exhibits the power of the superstructure to quickly identify both the optimal flowsheet and the optimal operational conditions under varying local seawater conditions. Finally, the third case study shows how the effect of certain parameters (e.g. RR) on plant performance could be systematically investigated through a repeated process of varying the value of the parameter in question and repeating the superstructure optimization. Since the superstructure allows the varying of both the hardware and flow patterns between different runs, this study allows designers to better gauge the impact of the parameter in question compared to traditional parametric and optimization studies.

An overview of the problem definition, which includes the objective func-

tions used as well as the mode of optimization, is presented in Section 2.4.1. The software utilized in this work, coupled with the solution methodology are outlined in Section 2.4.2.

#### 2.4.1 Problem Definition

The optimization problem considered herein is to determine both the optimal structure and the optimal operating conditions required to produce freshwater at the lowest possible cost. A multi-objective optimization is performed in the three case studies. Specifically, two different objective functions are chosen; one to represent the thermodynamic efficiency and the other to represent the economic costs. Maximizing thermodynamic efficiency is accomplished by maximizing the distillate production on a per unit of heating steam basis, a parameter known as the performance ratio (PR). Maximizing PR can also be thought of in terms of reducing operating costs of the plant, since less heating steam would be required to achieve a fixed freshwater production requirements. Minimization of costs is attained through the minimization of the specific heat transfer area requirements (SA) within the system. This is chosen as the preferred metric corresponding to capital costs. Although more detailed cost metrics could have been utilized, these are usually strongly dependent on prices which vary with geographical location and with time. It is useful to note that the methodology could be easily adapted to different relevant metrics. However, this might potentially result in optimization problems which are harder to solve.

The aforementioned multi-objective optimization problem is solved by reducing the problem to a series of single objective optimization problems [41, 42]. In each step, the PR is set prior to optimization. The optimization problem is reduced to finding the minimum SA required to satisfy the distillate production requirements. This same process is repeated for a series of different PRs. Ultimately, a Pareto frontier is formed which relate the minimum SA requirements for each PR, for wide span of different PRs. Each individual optimization represents a single data point on the Pareto frontier.

#### 2.4.2 Software and solution methodology

The superstructure was initially implemented using the JACOBIAN soft-ware package [43]. JACOBIAN is advantageous since it employs a simultaneous equation solver, which facilitates modeling by allowing the model equations to be inserted in whatever order is most intuitive, without the designer having to worry about the development of cumbersome algorithms to reach solution convergence. The only necessary condition is that the final set of equations is fully determined. The solver then identifies the equations and groups them into fully-determined blocks, which are subsequently solved iteratively to convergence. The accuracy of the generated model was verified by successfully reproducing the results attained by Zak, which in turn were validated against literature models [32].

The verified Jacobian model was then converted (using an in-house script) to an equivalent model implemented in General Algebraic Modeling System

(GAMS), a system suited for numerical optimization. GAMS was chosen since it is tailored for the optimization of complex, large-scale models and allows for the interface with numerous high-performance solvers [44]. To globally solve the non-linear problem of this study, the Branch-And-Reduce Optimization Navigator (BARON) was used. To facilitate model convergence, the generalized reduced gradient algorithm, CONOPT, is used as a local solver to quickly find an initial feasible solution within a few iterations [45, 46]. Theoretically, finding a global solution should be independent of the initial guesses. Practically speaking, however, it is found that faster and more probable convergence is attained when good initial guesses are provided. In addition to good initial guesses, it is especially important to have tight lower and upper bounds for each of the system variables; this helps significantly reduce the feasible space the optimizer has to navigate. Finally, to achieve a robust model, the model must be well scaled, with expected values for variables of around 1, (e.g. from 0.01 - 100 ). For instance, variables such as seawater salinity are preferably expressed as 4g/kg, as opposed to 40000 ppm which is often done in literature. Good initial guesses, sufficiently tight bounds of the variables as well as appropriate scaling are all ensured.

The model solution is difficult since the mathematical model involves many variables (more than 1200 variables) and many constraints (1150 equations and inequalities). Attaining good initial guesses for the final optimization model, the step necessary for an efficient solution procedure, was performed in a sequence of steps. The first GAMS optimization is run with zero degrees of

freedom which in essence is the equivalent of running a simulation. The attained variable values which are stored in an output file generated by GAMS become the initial guesses for the subsequent optimization. Instead of allowing the system all the proposed degrees of freedom at once which results in very high CPU requirements, the additional degrees of freedom are allowed to the system sequentially, whereby several equations are relaxed at a time. Each time additional degrees of freedom are made available to the system, the optimization is rerun using CONOPT, where the generated output file serves as the initial guesses for the next optimization run where more equations are relaxed. Once good initial guesses are determined, the final optimization is run using the global deterministic NLP solver Baron.

#### 2.4.3 Case study 1: Testing Different Design Specifications

Authors are not unanimous on what constitutes the optimal thermal structure. In fact, each has recommended different designs motivated by different design criteria. Proponents of the FF-MED arrangement have suggested alternative schemes. Some authors suggest that equal heat transfer areas in each of the effects is preferable, as in [47, 48]. This specification is projected to result in cost savings associated with buying identical units. Others have suggested a FF-MED scheme characterized by an equal drop in brine saturation temperature between effects [49], so as to minimize the area requirements. Proponents of the PC-MED arrangement propose different preferable conditions. These include fixing the concentration of the brine exiting each effect to the maximum allowable concentration; an arrangement intended to maximize overall

distillate production through maximizing RR within each effect [38]. Others specify near equal feed to each effect [15].

While each of the configurations has perceived advantages, this study compares the usefulness of each of the design criteria by comparing the performance of the optimal structure that satisfies the design requirements to the optimal structure attained by optimizing the superstructure with all its degrees of freedom. In each case, the design criteria are enforced by additional equations over and above the ones representing the model of the most general superstructure.

To ensure fair comparison among structures, the RR that all structures must satisfy is set. Since the feed entering into the effects must be pre-treated, setting a common RR ensures comparable pretreatment and pumping costs on a per unit of distillate basis. The optimization problem is then run according to described methods in Sections 2.4.1 and 2.4.2. Table 1 shows the comparison of the results attained under different specifications.

The results, as indicated in Table 1, confirm that for any particular distillate product requirement, the configuration arising from the superstructure optimization requires lower SA requirements than the optimal configuration arising from any of the proposed design specifications. This is expected given the additional degrees of freedom available to the unconstrained optimization, but nevertheless confirms that none of the already proposed structures are already optimal.

Design Specification	PR=10	PR=10.5	PR=11	PR=11.25
Unconstrained superstructure	389.2	403.0	427.4	469.4
General FF - MED	389.8	408.5	468.0	569.4
FF - MED with equal area within effects	395.4	408.9	469.1	582.5
FF - MED with equal temp. diff. between effects	392.1	410.6	468.6	583.4
PC - MED with near equal feed in all effects	431.4	418.9	438.7	485.8
PC - MED with max. brine salinity at effect exit	418.2	421.7	441.8	488.5

Table 1: Comparison of minimum SA requirements (m<sup>2</sup>/(kg/s)) for different design specifications for PR = 10, 10.5, 11 and 11.25 for  $T_{sw} = 25$  °C, Salinity = 4.2 g/kg, RR = 0.41

Table 1 indicates that the optimal general FF-MED (i.e., one without imposed constraints regarding equal areas or equal temperature differences) is a desirable structure for low distillate production requirements (PR=10, and PR = 10.5) since the SA requirements closely match those required by optimal structures arising from the unconstrained optimization. At higher distillate production requirements (PR = 11, and PR = 11.25), however, implementation of the FF-MED is not encouraged since the SA requirements exceed those of the superstructure by up to 21 percent. Table 1 further suggests that it is important to revise traditional design specifications such as imposing equal areas and equal temperature differences, which are shown to require slightly larger SA requirements (2 percent higher for PR = 11.25) than the general FF-MED configuration. Although equal areas within the effects may be more practical from an implementation standpoint, this practicality comes at the expense of extra area requirements; a trade-off that must be looked into in more depth by designers.

Table 1 indicates that the PC-MED with near equal feed entering each effect entering into each effect is optimal. The near equal feed constraint is imposed by dictating that none of 12 effects receives less than  $\frac{1}{15}$  of the total feed entering into the configuration. Still, results suggest that alternate structures motivated by the superstructure require significantly lower SA requirements at high PR requirements (3.5 percent reduction in SA requirements for PR = 11.5) .

## 2.4.4 Case study 2: Identifying optimal structures depending on location

Desalination plants extract seawater from varying bodies of water including the Mediterranean, the Red Sea and the Arabian Gulf, each of which is characterized by a different temperature and concentration. While experience in one area of the world could provide invaluable lessons applicable in other regions, the need to optimize configurations taking into account local conditions is irreplaceable. This case study identifies the optimal structure depending on the origin of seawater extraction for different PR requirements. For the sake of this study, constant nominal conditions are assumed according to [34]. Typically however, these conditions vary throughout the year, and ideally it would be best to optimize the structure taking into account the year round varying conditions. The superstructure in this case study is ensured to satisfy the form of a 12 effect MED, by adjusting the lower bounds of vapor production within each of the effects to an appropriate positive value.

	Standard	Mediterranean	Red Sea	Arabian Gulf
$T_{sw}$	20 ° C	26 ° C	28 ° C	26 ° C
$X_{sw}$	$3.5~\mathrm{g/kg}$	$3.8~\mathrm{g/kg}$	4.1 g/kg	$4.5~\mathrm{g/kg}$
PR = 10	359.2	388.3	413.6	403.8
PR = 10.5	371.0	402.3	428.2	418.7
PR = 11	392.8	429.0	457.6	453.4
PR = 11.25	422.4	467.6	501.1	515.0
PR = 11.5	590.6	667.8	758.2	963.5

Table 2: Comparison of minimum SA requirements (m<sup>2</sup>/(kg/s)) for different locations of seawater extractions; RR = 0.38,  $T_{HS_{input}}$  = 70° C

Results of this study, indicated in Table 6, suggest that for 12 effect MED structures, feed streams characterized by lower temperatures and concentrations require lower SA requirements. This may seem counter-intuitive since most of MED plants are installed in Saudi Arabia and the United Arab Emirates; countries which are mostly in contact with the Arabian Gulf. Moreover, countries with the seemingly favorable standard conditions have not exhibited significant installed MED capacities in recent times. Ultimately, however, the likelihood of implementation of a structure is a heavily influenced by the local fuel costs which are low in the Middle East, and the relative competitiveness of RO; a technology characterized by deteriorated performance at elevated salinity values. It is confirmed that the optimal configurations differ in the proposed flowsheet depending on the environmental conditions.

#### 2.4.5 Case study 3: Investigating influence of RR

For a fixed distillate production requirement, a higher RR results in lower overall flow of feed to the plant; and consequently both lower pretreatment costs and pumping requirements. Generally, whenever the maximum distillate production is desirable, the RR is maximized by designers insofar as scaling can be avoided. However, while increasing RR might increase distillate production, it has the disadvantages of increase SA requirements by increasing boiling point elevation losses. This study seeks to quantify the reduction in SA requirements (reducing capital costs) attained by reducing the RR constraint (increasing operating costs).

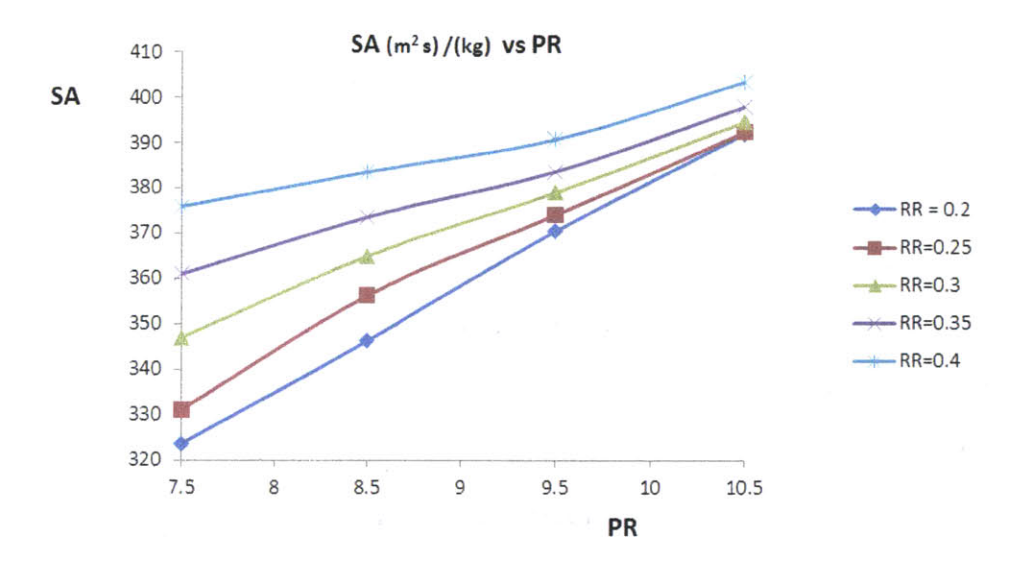


Figure 3: Comparison of minimum SA requirements  $(m^2/(kg/s))$  for different recovery ratios for 4 distillate production amounts

Figure 3 shows the results attained through this analysis for four differing PR requirements. It can be clearly seen that for a fixed PR, allowing for a decrease in required RR can result in significant decreases in SA requirements. This observation suggests that the ensuing reduction in capital costs might justify the additional operating costs the operators must tolerate. Ultimately

designers must weigh differing factors such as the cost of pre-treating the incoming feed (dependent on feed concentration), and the cost of different heat transfer areas before deciding which combination of optimal (PR, SA, RR) is preferable.

#### 2.4.6 Examples of optimal structures

While Section 2.4 illustrates that some non-conventional structures exhibit improved performance, this section presents the flow diagrams for some of prevalent optimal structures. The optimal structures for PR = 8.75 (Figure 4), PR = 10.25 (Figure 5) and PR = 11 (Figure 6), under the assumption of RR=40%, are all shown. The figures depict the optimal flow rates of all the different brine and feed streams, under the assumption of a 10 kg/s flow rate of input heating steam (not shown in the figure). Note that the absence of a particular preheater signals that all the vapor produced in the previous superstructure unit is sent in whole to the next effect.

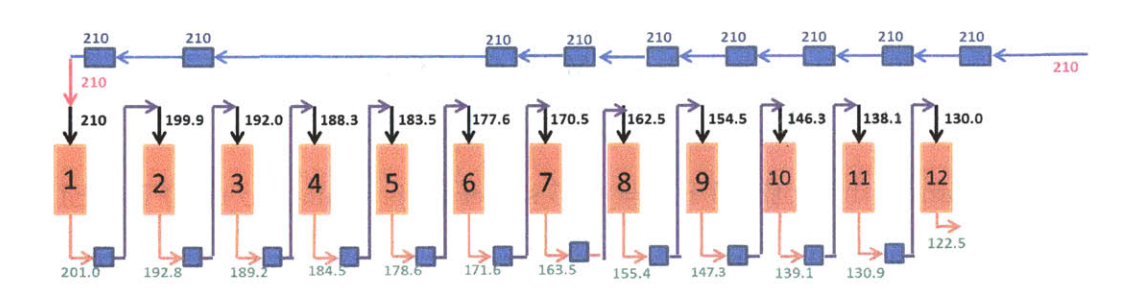


Figure 4: Optimized configuration for PR = 8.75

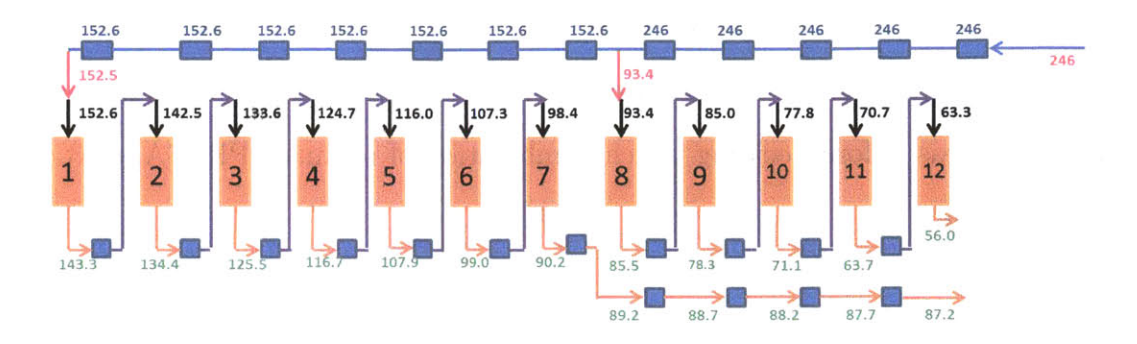


Figure 5: Optimized configuration for PR = 10.25

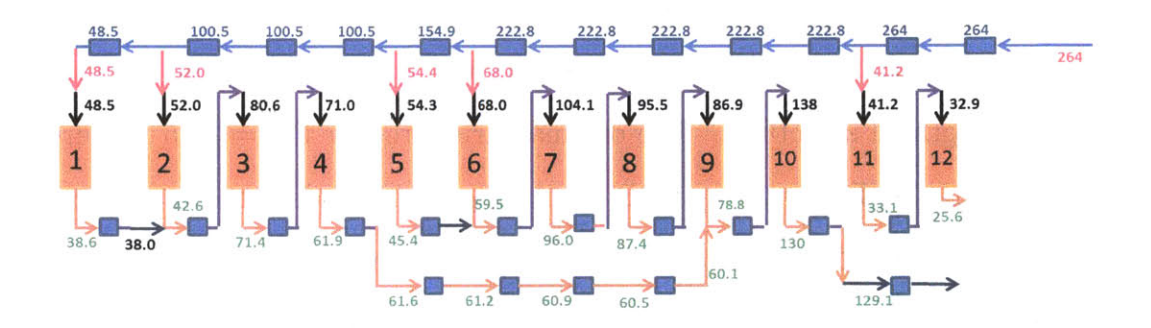


Figure 6: Optimized configuration for PR = 11

It can be seen that the presented structures are indeed non-standard, and do not follow any particular pattern with respect to how flows are directed. For this reason, it is difficult to clearly categorize these structures, although some of the structures do exhibit FF-MED and PC-MED like characteristics.

For instance, the optimal PR = 8.75 structure is similar to the FF-MED in the sense that no intermediate extractions occur. Moreover, all the brine outputted from the effects is completely redirected to the next effect. The optimal PR = 10.25 structure is interesting in that it resembles two FF-MED configurations connected in series. More precisely, the configuration is made

up of a 7 effect FF-MED structure connected to a 5 effect FF-MED. The feed entering the 7 effect FF-MED is pre-heated by the preheaters corresponding to the 5 effect FF-MED. Moreover, as indicated by Figure 5, the concentrated brine leaving the 7th effect is not inserted into any of subsequent effects, but rather flashed in a series of flash boxes to recover further energy from the brine. This action allows the 5 effect FF-MED to maintain lower outlet salinity brine at exit of its effects, which subsequently reduce boiling point elevation losses and thus reduce area requirements.

Compared to the lower PR structures, the optimal PR = 11 structure allows more frequent intermediate feed extractions from the main feed preheating line. The result is a lower amount of feed entering into the initial effects. The resulting reduction in sensible heating requirements allows for more vapor generation in the early effects, which ultimately increases the total distillate that can be formed in the structure. It is worthy noting the unconventional brine routing in the structure. For instance, the brine outputted in the 4th effect for instance is fed into the 10th effect, while the brine outputted from the 10th effect is allowed to by-pass all of the later effects.

A cursory look at the structure shows that optimization must be employed to obtain thermoeconomically favorable structures. For instance, a designer with the knowledge of the optimal structures corresponding to PR = 8.75 and PR = 10.25 would still not be able to accurately predict the optimal flowsheet for a structure corresponding to PR = 9.5.

#### 2.4.7 Conclusions

The capability of the superstructure in identifying improved stand-alone thermal structures has been demonstrated. Moreover, the superstructure is capable of:

- Testing different conventional design specifications. In addition to specifications investigated in case study 1, the superstructure model can be easily modified to allow for additional studies. One possible interesting study is to assess the merits and trade-offs associated with integrating thermal desalination plants with thermal vapor compression through a steam ejector. Another study could investigate the usefulness of subcooling the inputted heat steam; an effect designers claim has negligible effect on plant performance.
- Producing optimal off-design variations. If a plant is already in use,
   (i.e., component set and size of components are already specified), the
   superstructure could be easily adjusted to optimize operating conditions.
- Testing the sensitivity of configurations to relaxed technological constraints. For instance, if the top brine temperature is increased to 120°C instead of 70°C through improved anti-scalants, optimization of the superstructure can help identify how much improvement such a development would yield and would also inform the designers of the predicted flow patterns under the more favorable conditions. This sort of work, repeated for different possible constraints, can help identify which of the technological constraints are most limiting, a process which can help

optimally allocate funding for future R&D projects pertaining to thermal desalination. Mitsos et al. [50] utilizes a similar approach whereby a process superstructure was constructed to help compare hundreds of different alternatives for micropower generation. The developed model was subsequently used to test the sensitivity of system performance to variations in different parameters including operating temperature and physicochemical parameters.

Optimization of hybrid thermal-membrane technologies. Allowing the superstructure to be integrated with technologies such as RO and nanofiltration (NF) will likely identify new hybrid thermal-membrane technologies that will likely outperform an independent operation of the technologies.

Future work pertaining to modeling includes the implementation of more accurate seawater properties, including the introduction of a latent heat of evaporation/condensation of water that is temperature dependent as is done in [51]. Moreover, the effect of the number of repeating of superstructure units must be studied beyond the assumed 12 repeating units. For instance, approximately 40 stages are needed in order for MSF structures to realistically compete with MED structures in terms of distillate production. Moreover, the additional options of brine re-circulation and brine mixing can be afforded to the last unit within the superstructure, which enhances possibility of identifying improved structures.



# 3 Identifying Hybrid Configurations Involving TVC

#### 3.1 Introduction

The overwhelming need to overcome the world-wide problems relating to water scarcity has motivated diverse investigations aiming to enhance existing thermal desalination technologies. Recently, multi-effect distillation - thermal vapor compression (MED-TVC) systems with a top brine temperature lower than 70 °C have been gaining heightened attention as a potential improvement over the conventional MED structures [52, 53, 54, 55, 56, 57, 58].

The relative superiority of such integrated structures is especially noticeable in cogeneration schemes where only medium to high pressure heating streams (2-15 bar) are available from pre-existing power plants [59, 60]. In the most deployed MED-TVC scheme, a steam ejector utilizes the high pressure steam - known in this configuration as the motive steam - to entrain and subsequently compress a portion of vapor produced in the last MED effect. The resulting mixture, characterized by an intermediate pressure, is inputted as heating steam to the MED portion of the integrated plant, where it drives distillate production. For a fixed availability of motive steam at a specified pressure, this arrangement allows for the design of plants characterized by significantly larger distillate production capabilities (due to increased heating steam flow), coupled with reduced cooling water requirements on a per unit distillate basis [61]. This is in contrast to traditional MED plants which, constrained by the

low temperature operation required to minimize scaling, are unable to notably benefit from the higher exergy source, which implies an inefficient use of motive steam. Additional cited advantages include moderate investment costs, high reliability, easy operation and maintenance [62].

An abundance of steady-state mathematical models of the aforementioned MED-TVC desalination system have been developed as in [12, 15, 63, 64, 65, 66. These models were predominantly used to perform optimization studies seeking to determine preferable operating and design conditions for the system. Such investigations include examining the effect of factors such as the brine and intake seawater conditions, the number of effects, motive steam pressure and temperature, and the entrainment ratio on the total achievable distillate production of the plant. Other studies, however, have sought to fully optimize MED-TVC systems. Contrasting approaches include economic-based optimizations [60, 29, 67, 68], thermodynamic [53, 54, 69] and thermoeconomic optimizations [19, 70, 71]. In these studies, the main variables that are modified by the optimization process are the top brine temperature, the entrainment ratio and temperature differences between the effects. The structure of the thermal desalination plants, which inform how all the differing system flows are directed, are fixed prior to optimization. Most commonly a parallel feed MED arrangement whereby equal feed is inserted into each of the effects is assumed, as in [15, 54, 61]. Another is the forward feed MED. Moreover, while there are numerous modes of integrating the steam ejector with the thermal desalination system, most authors have narrowed their focus on optimizing schemes where the steam ejector compresses the vapors produced in the last effect of the MED.

One excellent study by Amer et al. [54] proposes such an alternate scheme whereby the steam ejector is used to compress a portion of the vapor produced in an intermediate effect, while the remainder of the vapor is used to drive another series of MED effects. The benefits of compressing vapor generated in an intermediate vapor is confirmed in a subsequent study by Koukikamali et al. [72] who, using a parametric study, conclude that the middle effects are better positions to locate suction port of the thermo-compressor in order to increase the gain output ratio and decrease the specific area. In both these studies, the routing of the flows is preset by the designers.

It is anticipated that the optimal flowsheet of the thermal desalination configuration - as part of an integrated system involving TVC - is different from that corresponding to a stand-alone thermal desalination configuration. Moreover, it is predicted that the optimal flowsheet highly depends on the location of vapor extraction. To the authors' knowledge, no optimization studies where the structure of the configurations in itself is a variable under investigation have already been carried out. This motivates the study proposed herein.

This chapter examines the advantages of intermediate thermal vapor compression by assessing its influence on several key parameters pertaining to both thermodynamic efficiency and economics. By doing so, desirable system characteristics system, such as the optimal location of vapor extraction, the optimal quantity of vapor to entrain and optimal ejector compression ratio, are pinpointed. The overall goal is to propose alternate improved integrated structures, possibly of unconventional flow patterns, that are capable of maximizing the synerigistic benefits of combining thermal desalination systems with thermal vapor compression systems.

#### 3.2 Problem definition

For fixed seawater conditions, the optimization problem proposed herein is to identify the optimal integrated configuration given a fixed flow-rate of motive steam available at a pre-determined pressure. The choice of these input parameters is presented in Table 3, although the study could be easily replicated for alternate choices of these parameters. In determining the optimal structure, the optimization problem is to determine all of the variables presented below:

- The choice of hardware components.
- The routing of brine, feed and vapor flows within the system.
- The sizing of the components including the effects and feed preheaters.
- The pressure within each of the effects and flash boxes.
- The choice of how much vapor to entrain in ejector.
- The pressure of entrained vapor.

Parameter	Value
Motive steam flowrate (kg/s)	10
Motive steam pressure (bar)	15
Seawater temperature (°C)	25
Seawater salinity (g/kg)	4.2

Table 3: Choice of parameters for present study including motive steam and seawater conditions.

Section 3.3 presents the model developed for the sake of this optimization, while Section 3.4 details the characteristics of the optimization, including the solvers used in addition to both the choice of objective functions and imposed constraints.

#### 3.3 Modeling

To enable the optimization procedure intended for this study, a flexible model of the integrated desalination and thermal compression plant is constructed. Section 3.3.1 presents a graphic illustration of the superstructure used to represent the different possible thermal desalination structures allowed in this chapter. Section 3.3.2 details the methodology used to integrate the thermal desalination model with the steam ejector, depending on choice of vapor extraction. Finally, Section 3.3.3 details the mathematical model used to represent performance of the steam ejector, detailing in the process the constraints required to satisfy proper operation.

#### 3.3.1 The thermal desalination superstructure

The thermal desalination superstructure utilized in this work is represented in Figure 7. While the superstructure can be used to represent any number of repeating units, the particular superstructure utilized in this work considers the specific example of 12 repeating units. Each theoretical unit is comprised of an effect, a preheater, a distillate flash box (not shown in figure for simplicity) and a set of brine flash boxes. It is important to clarify that just because a superstructure can represent a particular component does not mean that this particular component will be present in the finalized optimal structure. In fact, it will be observed in the results section, that only a subset of allowable components is usually necessary. Manipulation of component set in use is in principle controlled by the decision of what flow enters each component coupled with the decision of how to divide flows leaving a particular component. A detailed description of the different allowed flow options can be found in Chapter 2.

Ultimately, a very large amount of structures can be represented through the proposed superstructure. These not only include prevalent configurations such as the FF-MED and PC-MED, but also alternate non-conventional, yet potentially advantageous structures. Examples of potential structures include:

- An MED structure that transitions to an MSF structure.
- A FF MED structure that transitions to a PC structure.

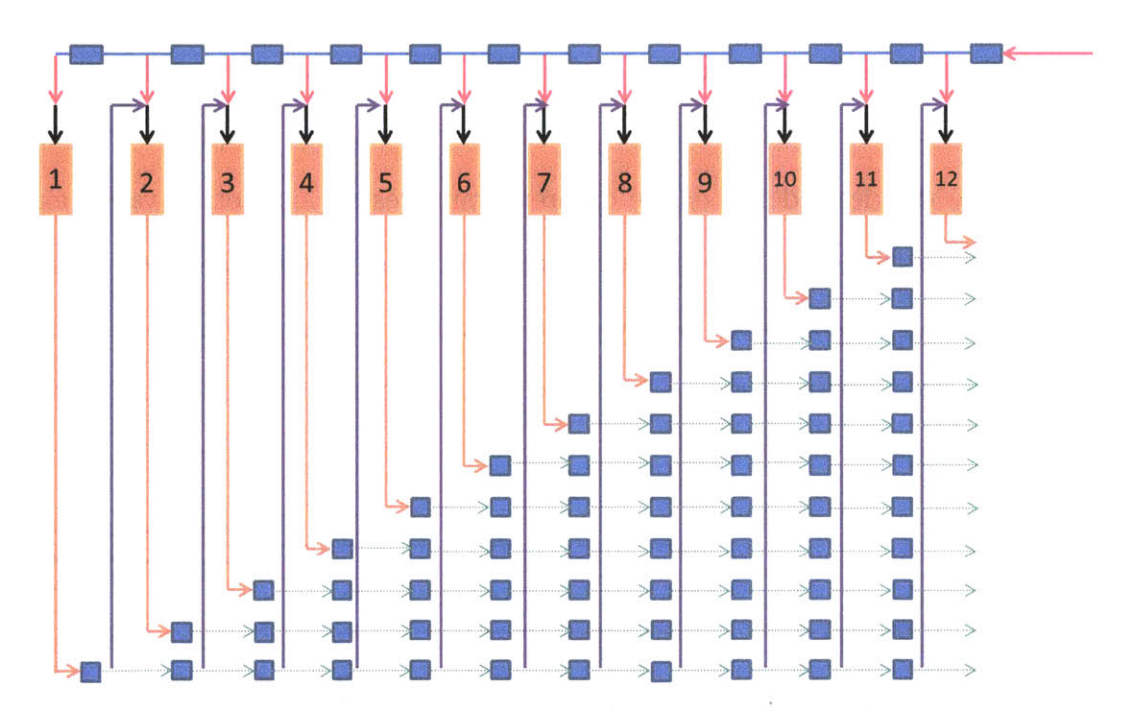


Figure 7: Superstructure capable of representing different combinations of MSF , MED and feed preheater combinations. Vapor routings are not represented in this schematic.

#### 3.3.2 Integration with steam ejector

To allow investigating whether the entrainment of a particular vapor stream is justified, the superstructure discussed in the prior chapter is modified. Within the unit where the extraction occurs, the updated model accounts for the fact that only a fraction of the unit's generated vapor is used as heating steam to the next unit. Moreover, the model modifies the flow-rate of heating steam to the 1st effect to account for the addition of entrained vapor over and above the incoming motive steam.

Herein, only the thermal compression of vapors produced in the 4th, 6th,

9th and the 12th (last) units is considered. While the analysis could be extended for vapors produced in any of the units, the proposed sample is sufficient to capture the dependence of the different variables on location of vapor extraction. To this end, four different models are constructed based on mass, energy and species balances for each of the possible system components. Sample schematics illustrating how vapor redirection occurs are shown in Figures 8 and 9.

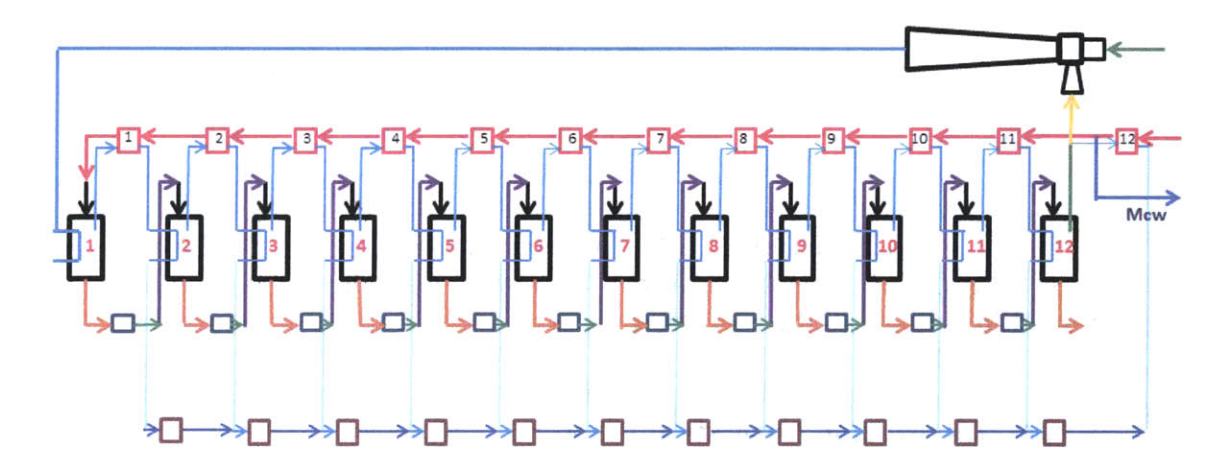


Figure 8: Example of FF MED - TVC configuration with vapor extracted from last effect. Only a fraction of the vapor generated in last unit needs to be condensed in the down-condenser.

#### 3.3.3 Model of the steam ejector

One critical step in studying the performance of the integrated systems is the evaluation of the performance of the steam ejector. Although numerous steam ejector models exist in the literature including [73, 74, 75, 76], the model used herein is based on the simple semi-empirical model proposed by Dessouky et al. [59, 77]. This model, in turn, is based upon extensive field

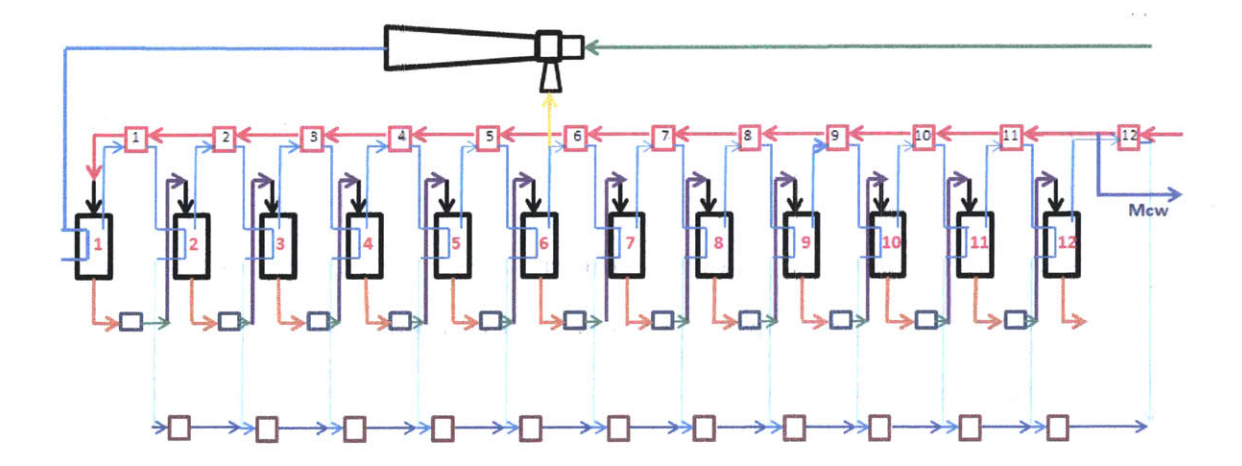


Figure 9: Example of a FF MED-TVC with vapor extracted from an intermediate (6th) effect. Only a fraction of vapor produced in the 6th unit is directed towards feed pre-heating and vapor production within the next (7th) unit.

data for compression ratio and entrainment ratio gathered by Power [78]. The particular correlation is chosen since it avoids lengthy computations of correction factors, which are conditional upon the pre-availability of a detailed design of the ejector.

The used model determines the required mass of motive steam to compress a unit mass of suctioned vapor (a parameter known as the entrainment ratio (Ra)). Ra can be computed for any given motive steam pressure  $(P_m)$ , suction pressure  $(P_{ev})$ , and desired discharge pressure  $(P_s)$  according to the relation below:

$$Ra = \frac{M_m}{M_{ev}} = 0.296 \frac{(P_s)^{1.19}}{(P_{ev})^{1.04}} \left(\frac{P_m}{P_{ev}}\right)^{0.015} \left(\frac{3 \times 10^{-7} (P_m)^2 - 0.0009 P_m + 1.6101}{2 \times 10^{-8} (T_{ev})^2 - 0.0006 (T_{ev}) + 1.0047}\right)$$
(1)

where  $T_s, T_m, T_{ev}$  refer to the temperatures of the discharge vapor streams, the motive steam and the entrained vapor, all expressed in  $^{\circ}$  C. All the pressure values are expressed in kPa.

Dessouky [59] further recommends the necessary conditions required to ensure normal, reliable and stable operation of the steam ejector. These are outlined below:

- Ra ≤ 4
- 10 ° C ≤  $T_{ev}$  ≤ 500°C
- -100 kPa $\leq P_m \leq 3500$  kPa
- $-~1.81 \leq Cr \leq 6$

where the compression ratio (CR) is defined as the pressure ratio of the discharge stream leaving the ejector to the vapor stream entrained in the ejector.

#### 3.4 Optimization

#### 3.4.1 Objective function

The profitability of operating a plant is of utmost importance when deciding to construct a particular plant. In desalination, the total generated

revenue is dependent not only on the quantity of water produced, but also the selling price of water. The main operating costs, on the other hand, are associated with the price of the total fuels required to supply heat to the thermal desalination plant. This in turn is dependent on local fuel costs, in addition to the quantity of fuel used. Finally the main capital costs are closely tied with the economics of construction of the flash boxes, the effects and the preheaters.

This chapter does not seek to delve into a detailed economic study, for the simple reason that the economics are dependent on many prices and costs that are location-dependent and time-variant. Moreover even the economic models already developed are acknowledged to have a high degree of uncertainty [65, 54]. Instead, price independent parameters are used in this work to allow comparison of different structures. The first parameter used is the gain output ratio (GOR), defined as the mass ratio of the total distillate production in the plant to the total input motive steam. Since the pressure of the motive steam is fixed in this study, the GOR is a useful metric which can be directly gauge the thermodynamic efficiency of a structure by quantifying distillate production from a fixed exergy input. In essence, the GOR relates the revenue generated in a plant to the operational costs associated with making steam available. The second parameter is the specific heat transfer area requirements (SA), defined as the total heat transfer area (within effects, feed preheaters and the down condenser) per unit distillate. The parameter approximates required capital investments to construct a plant. The drawback of the parameter is that it inherently assumes that the cost of heat transfer areas within an effect and

preheater are similar.

Literature ultimately compares different plants, which differ in both their production capabilities alongside their area requirements, thus rendering comparison between structures very cumbersome. A particular structure may result in higher GOR whereas another may require lower SA. To counter this problem, herein multi-objective optimization is performed whereby the GOR is maximized while the SA is minimized. A Pareto frontier is constructed which informs designers of the minimum SA for each GOR requirement. It is left to the designer to decide which of the numerous Pareto-optimal points is preferable.

#### 3.4.2 Optimization methodology

For each of the 4 models constructed, the multi-objective optimization approach implemented herein is approximated in a number of discrete steps. In each step the GOR is fixed prior to optimization, and SA are minimized for. The process is repeated for a range of GOR values. This discretization procedure in successful in reducing the problem to a series of single objective function optimization, thus enabling the use of black box solvers. All the models in this paper are developed in the General Algebraic Modeling System (GAMS), and globally optimized using BARON, a deterministic global algorithm capable of solving mixed integer non-linear programming problems [79, 80].

### 3.4.3 Constraints to allow justified comparison of different structures

The predominant structures that arise from different optimization problems can significantly differ. More specifically, feed and cooling water flows can vary drastically among structures, which would make comparing structures based on GOR and SA alone, without considering variation in other operating costs, unjustified. Larger feed and cooling water flows increase operational costs through elevating both pretreatments costs and system pumping requirements. To minimize large discrepancies between structures and allow for more fair comparison, additional constraints are imposed.

The first constraint imposes that the recovery ratio (RR) in any structure is greater than or equal to 0.2, where the RR is defined as the fraction of the total feed to the system (less the cooling water) that is converted to distillate. Note that to attain minimum SA, optimization favors minimum RR, as allowed by the value of the GOR imposed. This is because a lower RR lowers the average salinity of the brine leaving each effect, thus reducing boiling point elevation losses (BPE). Lower BPE losses in turn increase the prevalent temperature differential between the heating vapor and the brine being heated within each effect, thereby reducing area requirements. Low RR however detracts from distillate production capability of plants mainly by increasing feed sensible heating requirements, which alternatively could have been used to achieve further evaporation. Ultimately, for the lower GOR structures, the imposed inequality constraint is synonymous to setting the RR exactly to 0.2. For higher GOR

structures, the constraint allows optimization to resort to higher RR values that allow for satisfaction of distillate requirements. Caution however must be taken when comparing structures of differing RR's, where additional merit must be given to those structures with higher RR, all things else equal.

The second constraint imposes that the maximum allowable cooling water to total distillate ratio (CW-TD ratio) is set to 4. From an exergy accounting standpoint, allowing the brine blow-down to be outputted at a temperature very close to the seawater temperature is optimal. This arrangement however results in extremely large cooling water flow requirements. Generally availability of infinite cooling water can result in a simultaneous increase in distillate production (due to lower feed sensible heating requirements in last effect), and reduction in area requirements (larger possible average temperature difference between effects). Thus restricting the amount of cooling water on a per unit of distillate production basis is a good mechanism to maintain a realistic operating plant. Although the CW-TD constraint is introduced as an inequality constraint, it is generally always satisfied with equality by the optimizer.

#### 3.5 Results and discussion

### 3.5.1 Intermediate vapor extraction increases maximum possible GOR

For a fixed flow rate of motive steam at a predesignated pressure, results confirm that intermediate vapor extraction increases the maximum distillation production. Among the 4 extraction options allowed in this study, Table 4 in-

dicates that the maximum GOR is attained by the configuration with ES=9 which is capable of 35 percent more distillate production compared to the maximum achievable amount by the conventional MED-TVC. The next best alternative is the structure with ES=6, which itself is capable of achieving 10 percent additional distillate production. It is interesting to note that the optimal ES=4 structure is unable to match the distillate production capacity of the conventional MED-TVC, for reasons to be discussed later in the section. From an implementation standpoint, structures represented by maximum distillate production must be avoided as they require near infinite areas. It is still instructive however to use highlight prevalent features of these structures that enhance their distillate production capability.

ES	$GOR_{max}$	Ra	$P_{ev}$	CR	$Tv_{12}$	$T_{HS_1}$	$T_{HS_1}$ - $Tv_{12}$	RR
4	15.4	0.93	15.2	1.81	29.2	67.1	37.9	0.2
6	17.5	0.95	17.5	1.81	28.8	70.4	41.6	0.2
9	21.5	0.86	9.1	1.81	28.1	56.3	28.2	0.2
12	16	1.42	5.4	2.9	34.2	55.3	21.1	0.25

Table 4: Properties of maximum GOR structures for the different vapor extraction locations

To lay the foundation for the subsequent analysis, it is important to realize that integration with thermal vapor compression in the traditional MED-TVC increases GOR compared to the conventional MED precisely because it enables the reuse of the vapor produced in the last effect as heating steam to all the effects that precede it. It does so by first increasing the amount of heating steam available to the 1st effect. This increases vapor production in the 1st effect which in turn increases vapor production in the 2nd effect. This trend continues up until the last effect. For increased distillate production

goals, this is a much preferred scheme compared to the scheme common to the stand-alone MED, whereby most of the latent heat of the last effect vapor is transferred to cooling water that is eventually returned to the sea.

For a fixed supply of motive steam, it is intuitive that the entrainment of the largest amount vapor (i.e., low Ra) is desirable. Within steam ejectors, there is a prevalent trade-off between the amount of the low-pressure vapor that can be compressed, and the CR that results. Precisely, increasing amount of vapor entrained, decreases the CR. This analysis leads us to conclude that for the maximum GOR, the optimal structure should have the lowest allowable pressure ratio as allowed by ejector. The previously discussed lower bound on the CR is 1.81.

The downfall of the conventional MED-TVC is that it extracts vapor at the lowest system pressure corresponding to the pressure existing in the last effect. Assuming the last effect operates at a temperature slightly larger than the seawater temperature, a CR of 1.81 would result in a heating steam temperature that is not sufficiently elevated to drive a 12 effect MED. As an illustrative example, if the vapor pressure in the last effect is 4 kPa (corresponding to 30 °C temperature within the last effect), a CR of 1.81 would result in a heating steam temperature of approximately 40 °C. Given that the average BPE losses alone within each effect are approximately 0.8 °C, the total temperature difference is insufficient to drive heat transfer within 12 effects.

The intermediate vapor extraction scheme tackles this problem. By entraining vapors at higher pressures, it is possible to entrain the maximum amount of vapor as allowed by ejector operation. Table 4 confirms that for ES= 4, 6 and 9, the limiting factor to how much vapor can be entrained is the steam ejector operation limits, while for the case of ES= 12 the limiting factor is ensuring the optimal structure whereby there is both a sufficient temperature difference for heat transfer within each effect, while satisfying imposed constraints on how much cooling water can be utilized.

Variation in the maximum GOR among the different extraction locations can be attributed to the number of stages the entrained vapor is reused in. For the ES = 9 structure, the entrained vapor once compressed is used to generate additional vapor in the 1st effect through to the 9th effect. The 10th effect would generally receive the same amount of vapor had no compression between present in the system. For the ES=4 structure, however, the entrained vapor is only reused in 1st effect through to the 4th effect. This explains why the ES=4 structure, though capable of entraining more vapor, is still not capable of producing as much distillate as the conventional MED-TVC. In this light, it is predicted that for similar entrainment ratios, larger maximum GOR are possible for structures with the later extraction stage as is confirmed in Table 4.

## 3.5.2 Lower area requirements for structures with intermediate vapor compression

The performed study confirms that the location from where the vapor is extracted for entrainment is an important consideration that not affects the range of possible GOR, but also heavily influences the minimum SA requirements. Table 5 illustrates the results of the optimization of a 12 unit superstructure with vapor extractions from the 4th, 6th, 9th and 12th (last effect) respectively.

ES	GOR = 10	11	12	13	14	15	16	17	18	19
4	262	297	332	380	459	768	-	-	-	-
6	269	299	335	377	418	478	555	710	-	-
9	275	314	344	378	416	461	521	601	711	866
12	333	359	457	606	823	1217	3357	-	_	-

Table 5: Comparison of minimum SA  $(kgs)/(m^2)$  at different GOR for different ES.

Further, the choice of the optimal location of vapor extraction is highly dependent on exact GOR requirements. It is observed that for lower range of GOR requirements ( $10 \le \text{GOR} \le 12$ ), compression of a portion of vapor produced in 4th unit is most favorable (ES = 4). For the higher range of GOR requirements ( $13 \le \text{GOR} \le 16$ ), intermediate vapor extraction from later effects (ES=9) is most advantageous. For all GOR requirements, the conventional MED-TVC (ES= 12) is undesirable; it requires 27 additional % SA requirements compared to ES = 4 for GOR = 10, double the SA requirements compared to ES = 9 for GOR = 14, and more than six times the SA requirements compared to ES = 9 for GOR = 16.

Using the case of GOR = 15, Table 6 highlights important parameters that can be compared to understand variation in the SA requirements between structures dependent on their extraction location. The parameter  $\frac{T_{b_1} - T_{b_{ES}}}{ES - 1}$ computes the average temperature difference in the effects that precede the compression, while  $\frac{T_{b_{ES}}-T_{b_{N}}}{N-ES}$  computes the average available temperature difference in the possible effects/stages that follow vapor extraction. Finally,  $\frac{T_{b_1}-T_{b_N}}{N-1}$  is used to compute the average temperature difference in the entire structure. Knowing available temperature differences is important since they heavily influence area requirements and help inform choice of hardware. For instance, MSF stages can approximately double distillate production with double the temperature difference. To a first order, however, MED effects do not benefit from additional temperature differences from a distillate production standpoint, though required heat transfer areas are reduced with larger temperature differences. The optimization formulation weighs all different choices to first ensure distillate production requirements are met, and subsequently to ensure that it is done with the optimal component set that are least area intensive.

ES	Ra	CR	$T_{HS_1}$	$T_{v_{ext}}$	$T_{v_{12}}$	$\frac{T_{b_1} - T_{b_{ES}}}{ES - 1}$	$\frac{T_{b_{ES}} - T_{b_N}}{N - ES}$	$\frac{T_{b_1} - T_{b_N}}{N-1}$	SA
4	0.97	1.81	73.1	59.6	29.4	3.2	3.8	3.7	768
6	1.08	2.02	72.4	56.6	30.6	2.5	4.5	3.6	477
9	1.73	3.17	72.5	47.6	30.6	2.7	5.1	3.6	461
12	1.67	3.4	56.6	32.9	32.9	2.0	N/A	2.0	1217

Table 6: Properties of optimal structures for GOR = 15 for different vapor extraction locations

Intermediate vapor compression is found to reduce SA requirements for two main reasons. The first reason is that intermediate compression of vapor allows a larger fraction of the total heat transfer to occur in the initial effects (since more heating steam is available to the effects that precede extraction), which are characterized by highest overall heat transfer coefficients. This is in contrast to the conventional MED-TVC where near equal amount of heat transfer occurs in all effects. The second reason is that intermediate compression enables larger  $(T_{HS_1} - Tv_{12})$  factors as seen in Table 6, which allows a larger average temperature difference in the effects. This feature is possible since the compression of higher pressure streams allows a higher heating steam temperature to the first effect. Moreover, low brine blow down temperatures can still be maintained, since the uncompressed vapor is still capable of driving a thermal desalination whereby the last effect can approach temperature of seawater, as allowed by cooling water requirements.

#### 3.5.3 Optimal hybrid structures

The optimal hybrid structures take on varying forms depending on location of vapor extraction as indicated in both Tables 7 and 8. To the authors' knowledge, none of these structures have been previously proposed in the literature. A schematic of the MED-TVC + MED + MSF and the MED-TVC + MSF structures are presented in Figure 10 and 12 respectively, while a clarification of the routing of the different flows within each of structures as well as a justification of this naming is provided in Section 3.5.4. Simplified block-diagrams detailing the maximum GOR structures for ES = 6 and 9 can be found in

#### Appendix E.

ES	Structure
4	MED-TVC + MED + MSF
6	MED-TVC + MED + MSF
9	MED-TVC + MSF
12	MED-TVC

Table 7: Optimal structures corresponding to different ES for GOR = 15

ES	Structure
4	MED-TVC + MED + MSF
6	MED-TVC + MED + MSF
9	MED-TVC + MSF
12	MED-TVC

Table 8: Optimal structures corresponding to different ES for maximum GOR

#### 3.5.4 Flowsheets of optimal hybrid structures

Within any superstructure unit, the input heating steam can be directed in three alternative feasible ways. The first choice involves sending all of the heating steam to the MED effect where it is responsible for vapor production. The second feasible option is to utilize the heating steam exclusively for feed pre-heating purposes. The final option is to allow a fraction the heating steam to preheat the feed, while the other fraction is utilized to generate vapor in an MED effect.

The MED-TVC + MED + MSF structure, presented in Figure 10, is such a structure which utilizes all the aforementioned options. In the effects that precede the extraction, a typical MED structure results. All the discharge steam

exiting the steam ejector is directed towards vapor production in the 1st effect, while the intermediate generated vapors are split between feed pre-heating and vapor production. This part of the structure is referred to as the MED-TVC portion of the plant and includes both the steam ejector as well as all the effects leading up to and including the extraction stage. At the extraction stage, the generated vapor is split. The portion that is not entrained in the ejector serves as heating steam to a series of MED effects and their corresponding preheaters. This portion of the plant, made up of the unentrained vapor as well as the MED effects, is referred to as the MED portion of the plant. At a later stage, the structure transitions to yet another form, whereby all the generated vapor is dedicated solely for pre-heating purposes. This portion of the plant, which is devoid of any MED effects, produces vapor solely by brine and distillate flashing. As a result it is termed the MSF section of the plant. The integration of the three portions of the plant described is therefore termed the MED-TVC + MED + MSF structure. The MED-TVC + MSF structure, on the other hand, is represented in Figure 12. The MED-TVC section portion of the plant is similar to that described earlier. At the extraction stage, however, all the unentrained vapor is directed completely towards pre-heating the feed. This represents the MSF section of the plant.

For both structures, the vapor produced in the last MSF stage is cooled in a down-condenser, whereby additional cooling water is inserted to remove any additional heat that cannot be carried away by the incoming feed. Moreoever, for both structures, the routing of the feed is one such that all the incoming feed is inserted into one pre-heating line. Consequently, for the MED-TVC + MED + MSF structure, by the time the feed eventually enters into the MED-TVC section, it would already be significantly pre-heated by the vapor produced in both the MSF and the MED sections that follow it. Similarly, the feed that enters the MED section is preheated in the MSF section. For the MED-TVC + MSF structure, the feed entering MED-TVC section is preheated by the MSF structure. In both structures, the brine routing in the structures is such that the brine entering into the MSF stages is composed of brine streams exiting the earlier MED effects within the integrated structure.

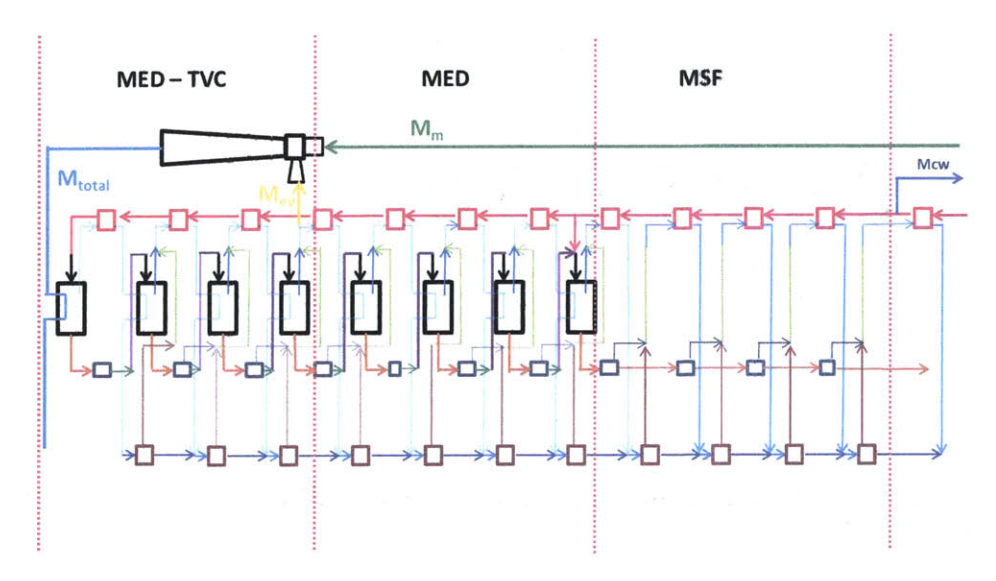


Figure 10: Illustration of example of an MED-TVC + MED + MSF with vapor extraction at N = 4

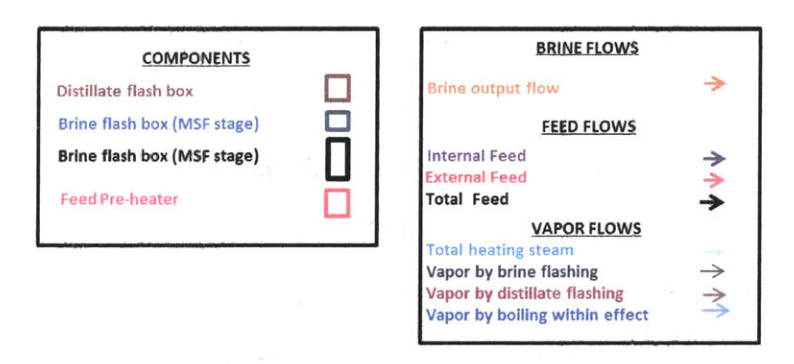


Figure 11: Labeling of different flow streams

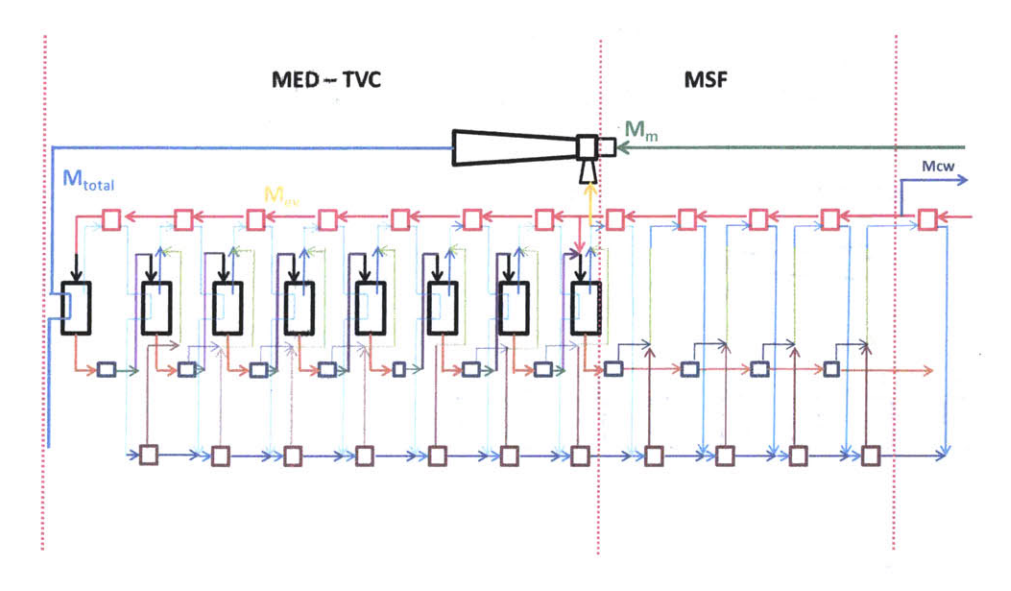


Figure 12: Illustration of an example of an MED-TVC + MSF with vapor extraction at N=8

#### 3.5.5 Advantages of hybrid structures

Numerous benefits are associated with the hybridized schemes proposed. For instance, the feed pre-heating requirements in the MED-TVC section are greatly reduced owing to the fact that the feed enters the MED-TVC section at a temperature significantly elevated compared to the seawater temperature. This has the implication of increasing the vapor production in the initial MED

effects, which translates into additional vapor production in the entire structure, thereby increasing GOR. Another notable advantage is that a significant reduction in the cooling water requirements is possible, resulting from the fact that only vapor produced by flashing in the last MSF section needs to be condensed, as compared to needing to condense the larger amount of vapor that would typically form in the more efficient boiling process which occurs with an MED effect. By setting a low temperature drop in the last MSF stage of both plants, it is possible to greatly reduce the vapor flow that needs to be condensed. Given that the cooling water requirements in this study are fixed, this arrangement enables a lower increase in the temperature of the feed as it flows through the down condenser. This is desirable since it allows the last effects and stages to operate at lower temperature conditions, which both increases thermodynamic efficiency and reduces SA requirements in system by increasing the average temperature difference in the effects.

Additional advantages include an increased production of vapor by distillate flashing in both the MED and the MSF sections, which is enabled by the large amount of distillate that is made available to the corresponding distillate flash boxes from the high distillate-producing MED-TVC section that precedes them. Finally, since the bulk of the total feed to the system is extracted to be fed to MSF stages, the pumping requirements are expected to be significantly lower than what they alternatively would have been had all the feed been directed to the 1st effect; an arrangement where pressure losses would be large owing to the large amount of brine circulation required. This however, cannot

be confirmed since pumping requirements are not directly computed in this work.

## 3.6 Conclusion

- Global optimization of a flexible superstructure, including the optimal selection of hardware, flow routings and operational conditions, enables the identification of two novel configurations the MED-TVC + MED + MSF and the MED-TVC + MSF which are capable of satisfying large GOR demands, with low area and cooling water requirements.
- For a fixed supply of heating steam, optimal structures with intermediate vapor compression are capable of significantly larger GOR compared to the conventional MED-TVC.
- For a fixed GOR, optimal structures with intermediate vapor compression are characterized by reduced SA requirements compared to conventional MED-TVC.
- There is no universally optimal location for vapor extraction. The optimal choice of extraction is dependent on the specific GOR requirement in question and can only be attained through a full optimization as performed in this study.

# Nomenclature

Variables	Name of Variable	$\operatorname{Units}$
T	Temperature	K
X	Salinity	g/kg
N	Flow variable	kg/s
$\mathbf{F}$	Feed to an effect	kg/s
HS	Heating steam to a superstructure unit	kg/s
V	Saturated vapor	
D	Distillate (saturated liquid)	
В	Brine exiting an effect	kg/s
Q	Rate of heat transfer	kJ/s
L	Latent heat of evaporation/condensation	kJ/kg
$c_p$	specific heat capacity at constant pressure	kJ/(kgK)

# Subscript

in	Input to a component
out	Output from a component
sat	Corresponding to saturation conditions of a component
i	Component number
ev	Entrained vapor
S	Discharge vapor
m	Motive steam
$\operatorname{ext}$	Extraction stage

# Superscript

BE	Brine evaporation within effect
BF	Brine flashing within brine flash box
DF	Distillate flashing within distillate flash box

## Abbreviations

FPH	Feed preheater	
EFF	Effect	
BFB	Brine Flash Box	
DFB	Distillate Flash Box	
BPH	Brine preheater	
RO	Reverse Osmosis	
NF	Nano filtration	
MSF	Multi-stage flash distillation	
MED	Multi-effect distillation	
Parameters	Name of Variable	Units
Parameters	Name of variable	Omis
Ra	Entrainment Ratio	Unitless
Ra	Entrainment Ratio	Unitless
Ra CR	Entrainment Ratio Compression Ratio	Unitless
Ra CR ES	Entrainment Ratio Compression Ratio Extraction Stage	Unitless Unitless

# Appendix

### Appendix A: Conventional Configuration Schematics

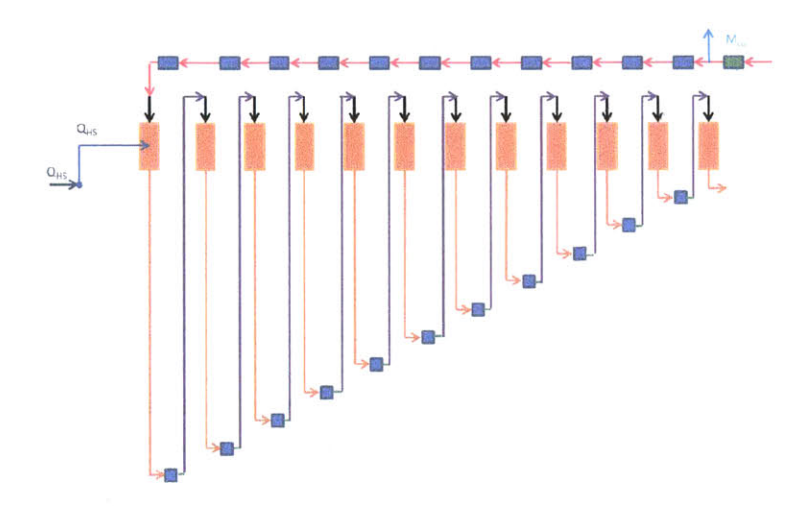


Figure 13: A 12 effect forward feed (FF) MED, from a simplified superstructure. (Brine and feed streams only)

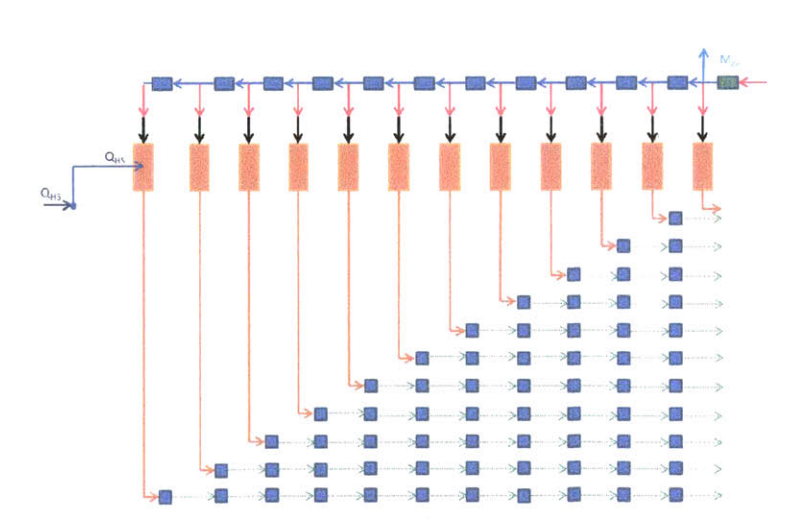


Figure 14: A 12 effect Parallel Cross (PC) MED, from a simplified super-structure (Brine and feed streams only). Brine flash boxes can be recursively removed to simplify to traditional PC MED.

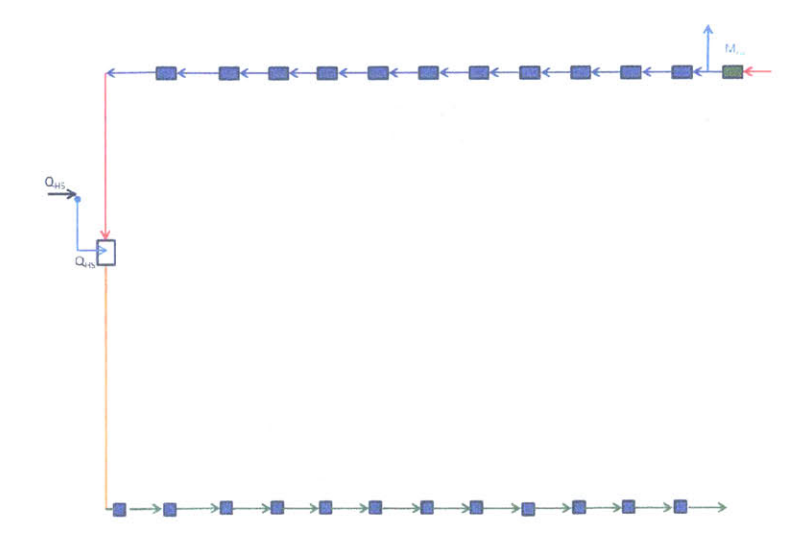


Figure 15: A 12 stage once through MSF, from a simplified superstructure. (Brine and feed streams only). Vapor generated in flash boxes is used to pre-heat the feed.

#### Appendix B: Mathematical Model

#### Mixer

Mixers have one output stream, but multiple input streams. Assuming m different incoming streams each characterized by an incoming mass flow rate  $N_{in_j}$ , the mass flow rate of the outputted stream  $N_{out}$  can be computed according to the relation:

$$N_{out} = \sum_{i=1}^{m} N_{in_j} \tag{2}$$

For the mixers dealing exclusively with liquid streams, the model assumptions of incompressible liquid streams and composition-independent enthalpies allow the energy balance to be simplified to:

$$T_{out} = \frac{\sum_{j=1}^{m} N_{in_j} T_{in_j}}{N_{out}}$$
 (3)

Moreover, when the composition of the different inlet streams is not identical, the salinity (X) of outlet stream can be computed from a species conservation balance as indicated below:

$$X_{out} = \frac{\sum_{j=1}^{m} N_{in_j} X_{in_j}}{N_{out}} \tag{4}$$

This work enforces that only saturated vapor streams of the same pressure can mix. For this reason, in the case of vapor mixers, the outlet stream is assumed to always be at the same temperature as the inlet streams.

#### Splitter

Splitters have one incoming stream, which is subsequently divided into 2 or more streams. Assuming an incoming stream  $N_{in}$  and m differing outgoing streams  $N_{out_j}$ , splitters are governed by a general mass conservation equations as described below:

$$N_{in} = \sum_{j=1}^{m} N_{out_j} \tag{5}$$

Assuming each outgoing stream is composed of a fraction  $\beta_j$  of original flow, any outgoing stream j can be expressed by relation below:

$$N_{out_j} = \beta_j N_{in}$$
 for j=1,2, ...., i (6)

where:

$$\sum_{j=1}^{i} \beta_j = 1 \tag{7}$$

#### MED effect

In MED effects, the mode of vapor production is brine evaporation, signaled by the superscript 'be'. In addition to the heat required to evaporate part of the brine, heat is also necessary to first sensibly heat the feed entering into an effect to the saturation temperature corresponding to the effect. Given a specified amount of heat entering into an effect i  $(Q_{eff_i})$ , the amount of formed vapor  $(V^{be})$  that can be formed is determined according to the energy balance in Equation 8.

$$Q_{eff_i} = F_i c_p (T_{sat_{eff_i}} - T_{feed_i}) + V^{be} L \tag{8}$$

#### Brine flashing box

In situations where saturated brine  $B_{bfb_{in}}$  is entered into a lower pressure brine flash box, the vapor generated by brine flashing  $(V^{bf})$  can be found as:

$$V^{bf} = \frac{B_{bfb_{in}}c_p(T_{sat_{in}} - T_{sat_{bfb}})}{L} \tag{9}$$

Subsequently, the amount of brine outputted from the flash box  $(B_{bfb_{out}})$  and its corresponding salinity  $(X_{bfb_{out}})$  are determined by a mass balance (Equation 10) and a salt balance (Equation 11) respectively.

$$B_{bfb_{out}} = B_{bfb_{in}} - V^{bf} \tag{10}$$

$$X_{bfb_{out}} = \frac{B_{bfb_{in}} X_{bfb_{in}}}{B_{bfb_{out}}} \tag{11}$$

The subscript 'bfb' refers to the brine flash box, while the superscript 'bf' refers to mode of vapor production, which corresponds to brine flashing.

Note: The brine flash boxes are chosen to operate at a similar pressure to that of the subsequent effect. This choice allows for the generated vapors to exit at similar pressures to the vapors generated within the effects, which allows for their mixing.

#### Distillate flashing box

Additional vapor is generated when saturated distillate at temperature  $T_{sat_{in}}$  is flashed in a lower pressure box operating at  $P_{sat_{dfb}}$ . This amount is found according to equation 12.

$$V^{df} = \frac{D_{dfb_{in}}c_p(T_{sat_{in}} - T_{sat_{dfb}})}{L} \tag{12}$$

The subscript 'dfb' refers to a distillate flash box component while the superscript 'df' refers to distillate flashing.

#### Preheater

In any particular feed preheater (FPH), a certain portion of heating steam condenses to provide the heat required to pre-heat the incoming feed. Assuming a specified amount of heat transfer  $Q_{FPH_i}$  is transferred to the incoming feed flow, the temperature of the feed at the outlet of the preheater can be determined according to Equation 13 below:

$$Q_{FPH_i} = F_{FPH_i}c_p(T_{FPH_{out}} - T_{FPH_{in}}) \tag{13}$$

#### Main Brine heater

Essentially also a feed preheater, the function of the main brine heater (MBH) function is to sufficiently heat the incoming feed such that the temperature of the outgoing feed exceeds the saturation temperature corresponding to the brine flash box into which the stream will be entered. This is necessary condition to induce brine flashing, the main mode of production within MSF configurations.

Assuming a total heat transfer of  $Q_{MBH}$  is transferred to the main brine heater, the temperature at the outlet of the device is determined according the energy balance in Equation 14.

$$Q_{MBH} = (F_{MBH})(c_p)(T_{MBH_{out}} - T_{MBH_{in}})$$

$$\tag{14}$$

#### Down Condenser

The down condenser (dc) is responsible for condensing the vapors generated in the last unit of the structure. This heat is carried away by seawater flowing through the down condenser  $F_{dc}$ , which is composed of both cooling water and total feed to rest of the thermal system. As such the amount of heat transfer can be expressed as:

$$Q_{dc} = HS_N L = F_{dc} c_p (T_{dc_{out}} - T_{sw})$$

$$\tag{15}$$

#### Appendix C: Heat transfer design equations

Design equations to compute the required heat transfer areas within the effects, the preheaters, the down-condenser and the brine heater are developed in this appendix. The heat exchanger areas are assumed to be just large enough condense the heating vapor incoming into the component.

Within the effects, the required heat transfer area  $A_{eff}$  is dependent on the overall heat transfer coefficient  $U_{eff}$  and the thermal temperature gradient and is computed as:

$$A_{eff_i} = \frac{Q_{eff_i}}{U_{eff_i} \Delta T_{eff_i}} \tag{16}$$

The thermal gradient  $\Delta T_{eff}$  within an effect is described by:

$$\Delta T_{eff_i} = T v_{i-1} - T_{eff_i} \tag{17}$$

The following relation gives the heat transfer area in the preheaters:

$$A_{FPH_i} = \frac{Q_{FPH_i}}{U_{FPH_i}LMTD_{FPH_i}} \tag{18}$$

where the log mean temperature difference in a preheater  $(LMTD_{FPH})$  is calculated as:.

$$LMTD_{FPH_{i}} = \frac{(Tv_{i} - T_{FPH_{i_{out}}}) - (Tv_{i} - T_{FPH_{i_{in}}})}{Ln\frac{(Tv_{i} - T_{FPH_{i_{out}}})}{(Tv_{i} - T_{FPH_{i_{in}}})}} = \frac{(T_{FPH_{i_{in}}} - T_{FPH_{i_{out}}})}{Ln\frac{(Tv_{i} - T_{FPH_{i_{out}}})}{(Tv_{i} - T_{FPH_{i_{in}}})}}$$
(19)

Similarly, the area requirements within the down-condenser can be computed as:

$$A_{dc} = \frac{Q_{dc}}{U_{dc}LMTD_{dc}} \tag{20}$$

where:

$$LMTD_{dc} = \frac{(T_{dc_{out}} - T_{sw})}{Ln\frac{(Tv_N - T_{sw})}{(Tv_N - T_{dc_{out}})}}$$
(21)

In the main brine heater, the are requirements are determined as:

$$A_{MBH} = \frac{Q_{MBH}}{U_{MBH}LMTD_{MBH}} \tag{22}$$

where LMTD across the main brine heater is found as a function of the temperature of input heating steam  $(T_{HS_0})$ , as:

$$LMTD_{MBH} = \frac{(T_{MBH_{out}} - T_{MBH_{in}})}{Ln\frac{(T_{HS_0} - T_{MBH_{in}})}{(T_{HS_0} - T_{MBH_{out}})}}$$
(23)

#### Appendix D: Model Assumptions

#### Thermodynamic assumptions

Given the narrow temperature range within which thermal desalination plants operate, several engineering approximations are justified. First, all liquid streams are considered incompressible. Moreover, a representative value of 4 kJ/kgK is assumed for the seawater specific heat at constant pressure  $(c_p)$ , which is assumed to be independent of temperature and salinity. Similarly, a constant enthalpy of evaporation of 2333 kJ/kg is assumed. Non-equilbrium allowance is assumed negligible [81, 82], while the boiling point elevation (BPE), which determines the variation in the saturation temperature of the brine and formed vapors due to their differing compositions, is computed according to accurate correlations developed by by Sharqawy et al [83]. These correlations are assumed to be dependent on both the composition and temperature of the saturated brine.

#### Further engineering assumptions

Several standard assumptions are used to derive the mathematical model. These include:

- Steady state operation.
- Negligible heat losses to the environment.
- Negligible pressure drops across the demister, the connecting lines and during condensation.
- Salt-free distillate (i.e., zero salinity).

- Negligible effect of non-condensable gases on system operation.
- Temperature-dependent overall heat transfer coefficients in both the effects and the preheaters computed according to [49]).
- To minimize the risk of scaling, the top brine temperature within effects is upper bounded at 70 °C, while the maximum allowable salinity is upper bounded at 72000 ppm.

# $\label{eq:appendix} \textbf{Appendix} \ \textbf{E}: \textbf{Block diagrams for maximum GOR structures involving TVC}$

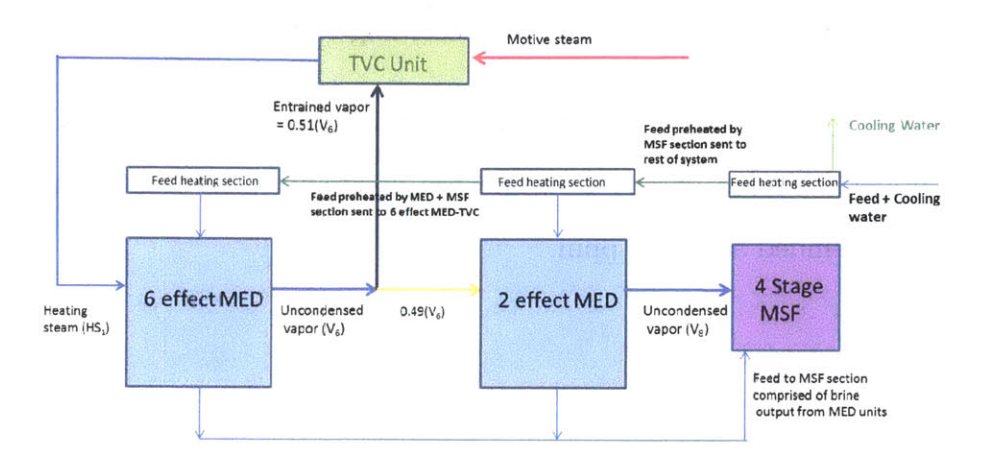


Figure 16: Simplified block diagram to illustrate make up of maximum GOR structure for  $\mathrm{ES}=6$ 

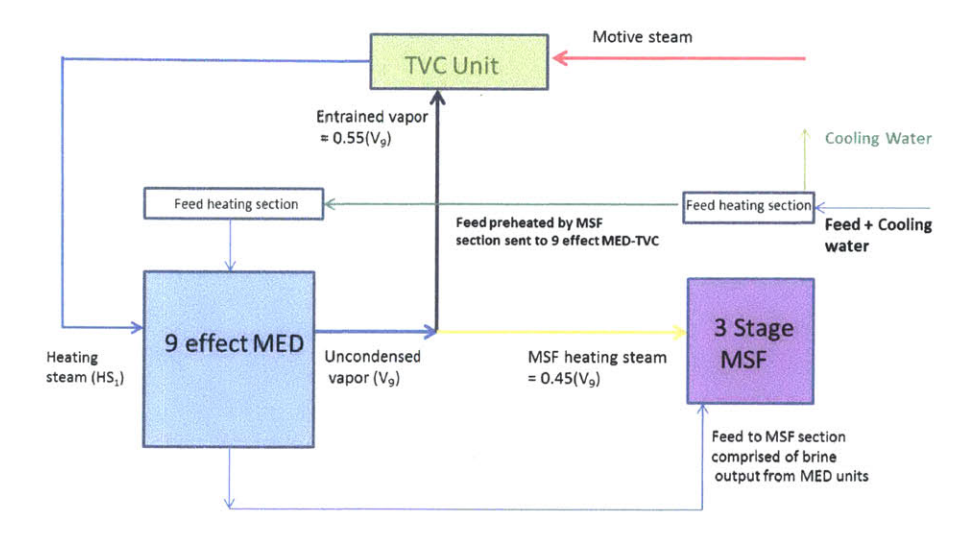


Figure 17: Simplified block-diagram to illustrate make up of maximum GOR structure for  $\mathrm{ES} = 9$ 

## References

- [1] T. Oki and S. Kanae. Global hydrological cycles and world water resources. *Science*, 313(5790):1068–1072, 2006.
- [2] C. J. Vorosmarty, P. Green, J. Salisbury, and R.B. Lammers. Global water resources: Vulnerability from climate change and population growth. Science, 289(5477):284–288, 2000.
- [3] United Nations Department of Economic and Social Affairs (UNDESA).

  Water scarcity. http://www.un.org/waterforlifedecade/scarcity.shtml.
- [4] Q. Schiermeier. Water: Purification with a pinch of salt. Nature, 452:260, 2008.
- [5] C. Fritzmann, J. Lowenberg, T. Wintgens, and T. Melin. State of the art reverse osmosis desalination. *Desalination*, 216:1–76, 2006.
- [6] M. Nair and D. Kumar. Water desalination and challenges: The middle east perspective: a review. Desalination and, 51:2030 – 2014, 2012.
- [7] A. A. Alawadhi. Pretreatment plant design key to a successful reverse osmosis desalination plant. Desalination, 110:1 - 10, 1997.
- [8] H. Ettouney and M. Wilf. Commercial Desalination Technologies. Green Energy and Technology, 2009.
- [9] M. M. Elimelech and W. A. Phillip. The future of seawater desalination: Energy, technology, and the environment. *Science*, 333:712–717, 2011.

- [10] M. A. Shannon, P. W. Bohn, M. Elimelech, J. G. Georgiadis, B. J. Marinas, and A. M. Mayes. Science and technology for water purification in the coming decades. *Nature*, 452:301–310, 2008.
- [11] A. H. Khan. Desalination Processes and Multistage Flash Distillate Practice. Elsevier, 1986.
- [12] D. Zhao, J. Xue, S. Li, H. Sun, and Q. Zhang. Theoretical analyses of thermal and economical aspects of multi-effect distillation dealing with high-salinity wasterwater. *Desalination*, 273:292–298, 2011.
- [13] H. T. El-Dessouky, I. Alatiqi, S. Bingulac, and H. M. Ettouney. Steadystate analysis of the multi-effect evaporation desalination process. Chemical Engineering & Technology, 21:15–29, 1998.
- [14] P. K. Sen, P. V. Sen, A. Mudgal, and S. N. Singh. A small scale multi-effect distillation (MED) unit for rural micro entrerprises part II - Paramteric studies and performance analysis. *Desalination*, 279:27–37, 2011.
- [15] F. Mandani, H. El-Dessouky, and H. M. Ettouney. Performance of parallel feed multiple effect evaporation system for seawater desalination. Applied Thermal Engineering, 20:1679 – 1706, 2000.
- [16] A. Jernqvist, M. Jernqvist, and G. Aly. Simulation of thermal desalination processes. *Desalination*, 134:187 – 193, 2001.
- [17] Y. M. El-Sayed. Design desalination systems for higher productivity. *Desalination*, 134:129–158, 2001.

- [18] S. E. Shakib, M. Amidpour, and C. Aghanajafi. A new approach for process optimization of ME-TVC desalination system. *Desalination and Water Treatment*, 37:84–96, 2012.
- [19] H. Sayyaadi and A. Saffari. Thermoeconomic optimization of multi effect distillation desalination systems. Applied Energy, 87:1122 – 1133, 2010.
- [20] C. Sommariva, D. Pinciroli, E. Sciubba, and N. Lior. Innovative configuration for multi stage flash desalination plant. IDA proceedings, San Diego, I:16, 1999.
- [21] S. F. Mussati, P. A. Aguirre, and N. J. Scenna. Novel configuration for a multistage flash-mixer desalination system. *Ind. Eng. Chem. Res.*, 42:4828–4839, 2003.
- [22] E. Cardona, S. Culotta, and A. Piacentino. Energy saving with msf-ro series desalination plants. *Desalination*, 153:167 171, 2003.
- [23] A. M. Helal. Hybridization a new trend in desalination. *Desalination* and Water Treatment, 3:120–135, 2009.
- [24] L. Awerbuch, V. van der Mast, and R. Soo-Hoo. Hybrid desalting systems
   a new alternative. Desalination, 64:51 63, 1987.
- [25] O. A. Hamed. Overview of hybrid desalination systems curent status and future prospects. *Desalination*, 186:207–214, 2005.
- [26] E. El Sayed, S. Ebrahim, A. Al-Saffar, and M. Abdel Jawad. Pilot study of MSF/RO hybrid systems. *Desalination*, 120:121–128, 1998.

- [27] M. G. Marcovecchio, S. F. Mussati, N. J. Scenna, and P. A. Aguirre. Global optimal synthesis of integrated hybrid desalination plants. Computer Aided Chemical Engineering, 26:573 – 578, 2009.
- [28] A. Messineo and F. Marchese. Performance evaluation of hybrid RO/MEE systems powered by a WTE plant. Desalination, 229:82–93, 2008.
- [29] H. Sayyaadi, A. Saffari, and A. Mahmoodian. Various approaches in optimization of multi eeffect distillation desalination systems using a hybrid meta-heuristic optimization tool. *Desalination*, 254:138–148, 2010.
- [30] H. Choi, T. Lee, Y. Kim, and S. Song. Performance improvement of multiple-effect distiller with thermal vapor compression system by exergy analysis. *Desalination*, 182:239 – 249, 2005.
- [31] L. T. Biegler, I. E. Grossmann, and A. W. Wasterberg. Systematic methods for Chemical Process Design. Prentice Hall, New York, 1997.
- [32] G. M. Zak. Thermal desalination: Structural optimization and integration in clean power and water. Master's thesis, MIT, 2012.
- [33] K. M. Sassi and I. M. Mujtaba. Effective design of reverse osmosis based desalination process considering wide range of salinity and seawater technology. *Desalination*, 306:8–16, 2012.
- [34] M. Skiborowski, A. Mhamdi, K. Kraemer, and W. Marquardt. Model-based structural optimization of seawater desalination plants. *Desalination*, 292:30 44, 2012.

- [35] S. F. Mussati, P. A. Aguirre, and N. J. Scenna. Improving the efficiency of the MSF once through (MSF-OT) and msf-mixer (MSF-M) evaporators. *Desalination*, 166:141 – 151, 2004.
- [36] S. F. Mussati, P. A. Aguirre, and N. J. Scenna. Superstructure of alternative configurations of the multistage flash desalination process. *Industrial Engineering Chemistry Research*, 45:7190–7203, 2006.
- [37] S. F. Mussati, P. A. Aguirre, and N. J. Scenna. Optimization of alternative structures of integrated power and desalination plants. *Desalination*, 182:123 129, 2005.
- [38] G. M. Zak and A. Mitsos. Hybrid thermal thermal desalination structures. *Desalination*, 2012.
- [39] S. F. Mussati, P. A. Aguirre, and N. J. Scennas. A rigorous, mixed-integer, nonlinear programming model (MINLP) for synthesis and optimal operation of cogeneration seawater desalination plants. *Desalination*, 166:339 – 345, 2004.
- [40] E. M. Ferreira. A. P. Balestieri and M.A. Zanardi. Optimization analysis of dual-purpose systems. *Desalination*, 250(3):936–944, 2010.
- [41] A. Pertsinidis, I. E. Grossmann, and G. J. McRae. Parametric optimization of MILP programs and a framework for the parametric optimization of MINLPs. Computers & Chemical Engineering, 22(Suppl):S205–S212, 1998.

- [42] D. Li, J. B. Yang, and M. P. Biswal. Quantitative parametric connections between methods for generating noninferior solutions in multiobjective optimization. *European Journal of Operation Research*, 117:84–99, 1999.
- [43] Jacobian modeling and optimization software. Numerica Technology, 2009.
- [44] A. Brooke, D. Kendrick, and A. Meeraus. GAMS: A User's Guide. The Scientific Press, 1988.
- [45] A. Drud. CONOPT A GRG code for large sparse dynamic nonlinear optimization problems. *Mathematical Programming*, 31(2):153–191, 1985.
- [46] A. Drud. CONOPT A large-scale GRG code. ORSA Journal on Computing, 6:207–216, 1992.
- [47] H. T. El-Dessouky and H. M. Ettouney. Fundamentals of Salt Water Desalination. Elsevier, 2002.
- [48] H. T. El-Dessouky and G. Assassa. Computer simulation of the horizontal falling film desalination plant. *Desalination*, 55:119 138, 1985.
- [49] H. El-Dessouky, I. Alatiqi, S. Bingulac, and H. Ettouney. Steady-state analysis of the multiple effect evaporation desalination process. *Chemical Engineering & Technology*, 21:437–451, 1998.
- [50] A. Mitsos, B. Chachuat, and P. I. Baron. Methodology for the design of man-portable power generation devices. *Industrial & Engineering Chem*istry Research, 46(22):7164-7176, 2007.

- [51] K. H. Mistry, M. A. Antar, and J.H. Lienhard V. An improved model for multiple effect distillation. *Desalination and Water Treatment*, 51:807– 821, 2013.
- [52] N. M. Al-Najem, M. A. Darwish, and F. A. Youssef. Thermo-vapor compression desalters: energy and availability analysis of single and multi-effect systems. *Desalination*, 110:223 228, 1997.
- [53] O. A. Hamed, A. M. Zamamiri, S. Aly, and N. Lior. Thermal performance and exergy analysis of a thermal vapor compression desalination system. *Energy Conversion and Management*, 37:379 – 387, 1996.
- [54] A. O. Bin Amer. Development and optimization of ME-TVC desalination system. Desalination, 249:1315 – 1331, 2009.
- [55] A. Al-Radif. Review of various combinations of a multiple effect desalination plant and a thermal vapour compression unit. *Desalination*, 93:119– 125, 1993.
- [56] S. E. Aly. Energy savings in distillation plants by using vapor thermocompression. *Desalination*, 49(S. E. Aly):37–56, Energy savings in distillation plants by using thermo-compression 1984.
- [57] T. Michels. Recent achievements of low temperature multiple effect desalination in the western areas of abu dhabi. *Desalination*, 93:111–118, 1993.
- [58] M. A. Darwish and A. Alsairafi. Technical comparison between TVC/MEB and MSF. *Desalination*, 170:223 239, 2004.

- [59] H. El-Dessouky. Modelling and simulation of the thermal vapour compression desalination process. Nuclear Desalination of Seawater, pages 315–338, 1997.
- [60] M. Shakouri, H. Ghadamian, and R. Sheikholeslami. Optimal model for multi effect desalination system integrated with gas turbine. *Desalination*, 260:254 – 263, 2010.
- [61] I. J. Esfahani, A. Ataei, V. Shetty, T. Oh, J. H. Park, and C. Yoo. Modeling and genetic algorithm-based multi-objective optimization of the MED-TVC desalination system. *Desalination*, 292:87 104, 2012.
- [62] F. Al-Juwayhel, H. El-Dessouky, and H. Ettouney. Analysis of single-effect evaporator desalination systems combined with vapor compression heat pumps. *Desalination*, 114:253–275, 1997.
- [63] R. K. Kamali, A. Abbassi, and S. A. Sadough. A simulation model and parametric study of MED-TVC process. *Desalination*, 235:340 – 351, 2009.
- [64] F. N. Alasfour, M. A. Darwish, and A. O. Bin Amer. Thermal analysis of ME-TVC+MEE desalination systems. *Desalination*, 174:39 61, 2005.
- [65] M. Al-Salahi and H. Ettouney. Developments in thermal desalination processes: Design, energy, and costing aspects. *Desalination*, 214:227 – 240, 2007.
- [66] K. A. Ahmed and O. A. Hamed. An assessment of an ejectocompression desalination system. *Desalination*, 96:103–111, 1994.

- [67] M. A. Sharaf, A. S. Nafey, and L. Garcia-Rodrigues. Exergy and thermoeconomic analyses of a combined solar organic cycle with multi effect distillation (med) desalination process. *Desalination*, 272:135–147, 2011.
- [68] N. Lukic, A. P. Froba, L. L. Diezel, and A. Leipertz. Economical aspects of the improvement of a maechanical vapor compression desalination plant by dropwise condensation. *Desalination*, 264:173–178, 2010.
- [69] R. K. Kamali, A. Abbasi, S. A. Vanini, and M. S. Avval. Thermodynamic design and parametric study of MED-TVC. *Desalination*, 222:596–604, 2008.
- [70] K. Ansari, H. Sayyaadi, and H. Amidour. Thermoeconomic optimization of a hybrid pressurized water reactor (PWR) power plant coupled to a multi effect distillation system with thermo-vapor compressor (med-tvc). Energy, 35:1981–1996, 2010.
- [71] J. Ghelichzadeh, R. Derakhshan, and A. Asadi. Application of alternative configuration of cogeneration plant in order to meet power and demand. *Chemical Engineering Transactions*, 29:775–780, 2012.
- [72] R. Koukikamali, M. Senaei, and M. Mehdizadeh. Process investigation of different locations of thermo-compressor suction in med-tvc plants. *De*salination, 280:134–138, 2011.
- [73] H. El-Dessouky, H. Ettouney, L. Alatiqi, and G. Al-Nuwaibat. Evaluation of steam jet ejectors. Chemical Engineering and processing, 41:551–561, 2002.

- [74] N. H. Aly, A. Karameldin, and M. M. Shamloul. Modelling and simulation of steam jet ejectors. *Desalination*, 123:1–8, 1999.
- [75] R. K. McGovern, G. P. Narayan, and J. H. V. Lienhard. Analysis of reversible ejectors and definition of an ejector efficiency. *Internation Journal of Thermal Sciences*, 54:153–166, 2012.
- [76] A. Arbel, A. Shklyar, D. Hershgal, M. Barak, and M. Sokolov. Ejector irreversibility charecteristics. *Journals of Fluids Engineering*, 125:121– 129, 2003.
- [77] H. T. El-Dessouky, H. M. Ettouney, and F. Al-Juwayhel. Multiple effect evaporation vapour compression desalination processes. Chemical Engineering Research and Design, 78:662 – 676, 2000.
- [78] B. R. Power. Steam jet ejectors for process industries. McGraw-Hill's, 1:1-494, 1994.
- [79] N. V. Sahinidis. BARON: A general purpose global optimization software package. *Journal of Global Optimization*, 8(2):201–205, 1996.
- [80] M. Tawarmalani and N. V. Sahinidis. A polyhedral branch-and-cut approach to global optimization. *Mathematical Programming*, 103:225–249, 2005.
- [81] K. H. Mistry, M. A. Antar, and J. H. Lienhard V. An improved model for multiple effect distillation. *Desalination and Water Treatment*, 51(aheadof-print):807–821, 2013.

- [82] P. Druetta, P. Aguirre, and S. Mussati. Optimization of multi-effect evaporation desalination plants. *Desalination*, 311:1 15, 2013.
- [83] M. H. Sharqawy, J. H. Lienhard V, and S. M. Zubair. Thermophysical properties of seawater: A review of existing correlations and data. *De*salination and Water Treatment, 16:354–380, 2010.